Coupled Systems Mechanics, *Vol. 9, No. 3 (2020) 237-264*
DOI: https://doi.org/10.12989/csm.2020.9.3.237

Bending behaviour of FGM plates via a simple quasi-3D and 2D shear deformation theories

Ali Youcef[1,2], Mohamed Bourada[1], Kada Draiche[1,3], Belhadj Boucham[2], Fouad Bourada*[1,4] and Farouk Yahia Addou[1]

[1]Material and Hydrology Laboratory, Faculty of Technology, Civil Engineering Department, University of Sidi Bel Abbes, Algeria
[2]Laboratory of Mechanics of Structures and Solids (LMSS), Faculty of Technology, Department of Mechanical Engineering, University Sidi Bel Abbes University, Algéria
[3]Département de Génie Civil, Université Ibn Khaldoun Tiaret, BP 78 Zaaroura, 14000 Tiaret, Algérie
[4]Département des Sciences et de la Technologie, Centre Universitaire de Tissemsilt, BP 38004 Ben Hamouda, Algérie

(Received March 12, 2019, Revised October 29, 2019, Accepted January 1, 2020)

Abstract. This article investigates the static behaviour of functionally graded (FG) plates sometimes declared as advanced composite plates by using a simple and accurate quasi-3D and 2D hyperbolic higher-order shear deformation theories. The properties of functionally graded materials (FGMs) are assumed to vary continuously through the thickness direction according to exponential law distribution (E-FGM). The kinematics of the present theories is modeled with an undetermined integral component and satisfies the free transverse shear stress conditions on the top and bottom surfaces of the plate; therefore, it does not require the shear correction factor. The fundamental governing differential equations and boundary conditions of exponentially graded plates are derived by employing the static version of principle of virtual work. Analytical solutions for bending of EG plates subjected to sinusoidal distributed load are obtained for simply supported boundary conditions using Navier'is solution procedure developed in the double Fourier trigonometric series. The results for the displacements and stresses of geometrically different EG plates are presented and compared with 3D exact solution and with other quasi-3D and 2D higher-order shear deformation theories to verify the accuracy of the present theory.

Keywords: E-FGM; static behaviour; quasi-3D; shear deformation; bending

1. Introduction

The composite structures possess a great number of chemical, mechanical and other types of properties, such as the stiffness and strength that provide the structure with the ability to maintain its shape and dimensions under loading or any other external action. However, these properties are a function not only of their basic constituents, but also the quality of the connection between fiber and matrix or layer and layer. Indeed, the interface, or more precisely the interfacial zone, is very complex and plays an essential role in the mechanical strength of composite materials, because it represents a zone of accumulation and stress concentration that can strongly influence the behaviour

*Corresponding author, Ph.D., E-mail: bouradafouad@yahoo.fr

http://www.techno-press.org/?journal=csm&subpage=8 ISSN: 2234-2184 (Print), 2234-2192 (Online)

of composite structures. However, in order to avoid interfacial debonding, matrix cracks and other damage mechanisms found at the interface of laminated composite and sandwich plates, the material scientists have been involved in the design of materials that perform better than conventional composites to optimize their resistance to damage, usually with much higher chemical and mechanical properties and excellent fiber/matrix adhesion.

Recently, a new class of composite materials known as functionally graded materials (FGMs) has been proposed and has attracted a great amount of attention from researchers in many fields, including aerospace, nuclear reactor, biomaterial industry, environmental sensors and other engineering applications areas. Moreover, functionally graded material (FGM) is an advanced composite material that can be used in high temperature environments. This material is obtained by mixing two different materials, typically made of metal and ceramic, in which the volume fractions of the constituents change gradually and continuously from one surface to another, which is totally different from the conventional composite materials. In technical world the concept of FGMs was first proposed by a research group around 1984 in Japan during a space plane project. In this case, the combination of materials is initially designed as thermal barrier for aerospace structural applications and fusion reactors and is able to withstand a surface temperature of about 2000 K and a temperature gradient of approximately 1000 K as described by Mahamood and Akinlabi (2017). In recent years, these research activities have spread not only in Japan but also around the world, particularly in Germany and the United States. The development of (FGMs) and its various specific applications in the different fields of industry can be found in the literature by several authors (Koizumi 1993, 1997, Kawasaki and Watanabe 1997, Pindera *et al*. 1997, Muller *et al*. 2003, Schulz *et al*. 2003, Pompe *et al*. 2003, Kumar 2010, Gandra *et al*. 2011, Zhao *et al*. 2012, Ahmed 2014, Kar and Panda 2015, Kolahchi *et al*. 2015, Daouadji *et al*. 2016, Miyamoto 2016, Aldousari 2017, Avcar and Alwan 2017, Faleh *et al*. 2018, Akbaş 2018a, Eltaher *et al*. 2018, Avcar and Mohammed 2018, Karami *et al*. 2018, 2019a, b, Avcar 2019, Alimirzaei *et al*. 2019, Boutaleb *et al*. 2019, Hussain and Naeem 2019).

With the increased use of these advanced composite materials, various researches of many authors throughout the world have been tried about the modeling and engineering applications of FGMs. For this purpose several plate theories have been developed to predict accurately the bending, buckling and vibration behaviours of FG plates. Reddy (2000) presented a theoretical formulation and finite element models including geometric non-linearity based on the third-order shear deformation theory for the static and dynamic analysis of thick FG plates subjected to mechanical and thermal loads. Then, Cheng and Batra (2000) used also Reddy'is third order plate theory to present the critical buckling load and vibration frequency results of the functionally graded polygonal plates resting on a Winkler-Pasternak elastic foundation and subjected to uniform in-plane hydrostatic loads. Javaheri and Eslami (2002) obtained the equilibrium and stability equations based on the classical plate theory for the buckling analysis of FG plates subjected to distributed linear and nonlinear thermal load. Vel and Batra (2004) presented a 3-D exact solution for the free and forced vibration of simply supported thick FG plates in which the material properties of the constituent are estimated to vary gradually in the thickness direction of the plate by employing the Mori-Tanaka or the self-consistent schemes. Qian *et al*. (2004) analyzed the static and dynamic responses of thick rectangular FG plates by using a compatible higher-order shear and normal deformable plate theory together with a meshless local Petrov-Galerkin (MLPG) method. Ferreira *et al*. (2005) used the meshless collocation method based on the multiquadric radial basis functions and a third-order shear deformation theory to analyze the static deformations of FG square plates. In thus analysis two homogenization techniques have been utilized to determine effective material properties of the composite. A simply supported elastic rectangular FG plate subjected to transverse loading is investigated by Chi and Chung (2006). The material properties of the FGM plates are assumed to vary continuously in the thickness direction by three different distributions; power-law (P-FGM), sigmoid (S-FGM), and exponential (E-FGM) plates. Their analysis carried out, bases on the classical plate theory and the series solutions of the FGM plates are obtained by expanding the transverse load into Fourier series expansion. Analytical solution for bending response of simply supported FG plates subjected to a transverse uniform load is obtained by Zenkour (2006) using a generalized shear deformation theory and the Navier solution procedure.

In the last few years, functionally graded material plates modeling, characterization and analysis are carried out by Birman and Byrd (2007). They presented the principal developments, fabrication, design and applications of FGMs concentrating on the recent research published since 2000. Carrera *et al*. (2008) employed the unified formulation and the principle of virtual displacements to obtain finite element solutions for the static analysis of FG plates subjected to transverse mechanical loadings. Jha *et al*. (2013) reviewed the various investigations carried out in the existing literature for the stress, free vibration and buckling analyses of FG plates reported in the recent works published since 1998. This review is intended to give the readers a feel for the variety of studies and applications related to graded composites. Daouadji and Hadji (2015) presented and analytical solution of nonlinear cylindrical bending for functionally graded plates. Nguyen *et al*. (2015) proposed a refined hyperbolic higher-order shear deformation theory with four unknowns for bending, vibration and buckling analysis of FG sandwich plates with homogeneous hardcore and soft core. Laoufi *et al*. (2016) investigated the mechanical and hygrothermal behaviour of FG plates using a hyperbolic shear deformation theory. Rezaiee-Pajand *et al*. (2018) discussed the static response of FG non-prismatic sandwich beams. Lal *et al*. (2017) studied the thermo-mechanically induced finite element based nonlinear static response of elastically supported functionally graded plate with random system properties. Therefore, the development of various models for the modeling and global responses of FG plates and shells under mechanical and thermal loadings based on the equivalent single layer theories (CPT, FSDT, TSDT and HSDTs), the exact elasticity solution and the unified formulation have been comprehensively reviewed in detail by Thai and Kim (2015). Thom *et al*. (2017) utilized an accurate computational approach based on finite element method and a new third-order shear deformation plate theory for static bending and buckling behaviours of 2D-FGM plates under statically mechanical loading. The effective properties are assumed to be graded in two directions and are computed using the rule of mixture. It should be noted that some HSDTs are presented in literature for studying the mechanical behaviors of structures with and without experimental investigations (Mehar and Panda 2016, 2018, Bisen *et al*. 2018, Mehar and Panda 2019, Singh *et al*. 2019, Mehar *et al*. 2019, Batou *et al*. 2019, Boulefrakh *et al*. 2019, Karami *et al.* 2019e, Salah *et al*. 2019, Tounsi *et al*. 2020).

Currently, many studies and numerical investigations related to quasi-3D HSDTs have been carried out and available in literature to study the effect of thickness stretching in plates and shells structures made by FGMs. For instance, Neves *et al*. (2013) proposed the quasi-3D higher-order shear deformation theory rest on a unified formulation coupled with radial basis functions for the static, free vibration and buckling analyses of FG isotropic plates and FG sandwich plates. A simple and accurate quasi-3D trigonometric plate theory (TPT) with 5-unknowns is employed by Mantari and Guedes Soares (2014) for the bending analysis of advanced composite single layer and sandwich plates subjected to bi-sinusoidal load for simply supported boundary conditions. Vo *et al*. (2015) presented a finite element model by using a quasi-3D theory to investigate the free vibration and buckling analyses of FG sandwich beams with FG skins-homogeneous core and homogeneous skins-FG core. From this study the thickness stretching effect on natural frequencies and critical buckling of sandwich beams for various power-law indexes was also analyzed. Analytical solutions for bending analysis of composite beams made of isotropic materials, fibrous composite materials and FGMs are presented by Shinde and Sayyad (2017) using a quasi-3D polynomial shear and normal deformation theory. In recent times, Zaoui *et al*. (2019) used new 2D and quasi-3D shear deformation theories for free vibration of FG plates on elastic foundations. Mahmoudi *et al*. (2019) employed a refined quasi-3D shear deformation theory for thermo-mechanical behavior of FG sandwich plates on elastic foundations. Khiloun *et al*. (2019) presented an analytical modeling of bending and vibration of thick advanced composite plates using a four-variable quasi 3D HSDT.

This paper presents a new simple quasi-3D and 2D hyperbolic higher-order shear deformation theories (HySDT) for static analysis of EG plates. The advantage of these theories is that the displacement field is modeled with only four unknowns (ε_z=0) or five unknowns ($\varepsilon_z \neq 0$), which is even less than the other quasi-3D and 2D shear deformation theories and do not require shear correction factor. The mechanical properties of the plates are assumed to vary continuously through the thickness direction according to exponential law distribution (E-FGM) in terms of the volume fractions of the constituents. The governing equations of the EG plates and its boundary conditions are derived by employing the principle of virtual work. Navier-type analytical procedure is obtained for EG plates subjected to transverse sinusoidal load for simply supported boundary conditions. The numerical results obtained by the proposed model for axial and transverse displacements and stresses of very thick, thick and moderately thick rectangular EG plates are verified by comparing them with that of the results of other 2D and quasi-3D shear deformation theories.

2. Theoretical formulation

2.1 Exponentially graded plates

Consider a rectangular FG plates with uniform thickness h, length a and width b, made of a mixture of metal and ceramic materials and referred to the rectangular Cartesian coordinate system (x, y, z) as depicted in Fig. 1. In this analysis the Poisson ratio, v is assumed to be constant, whereas, the effective material properties, such as Young'is modulus E vary exponentially through the thickness of the plate according to the volume fractions of the constituents or so-called the exponential function (see Fig. 2) and as indicated in the following equation

$$E(z) = E_b V(z), \qquad \mathrm{V}(z) = e^{p\left(\frac{z}{h}+\frac{1}{2}\right)} \tag{1}$$

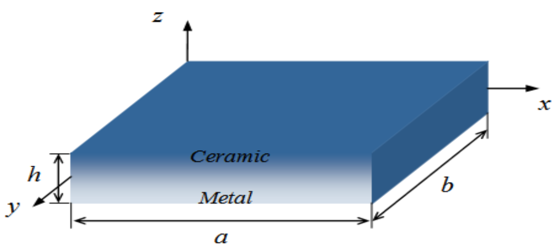

Fig. 1 Geometry of an exponentially graded plate

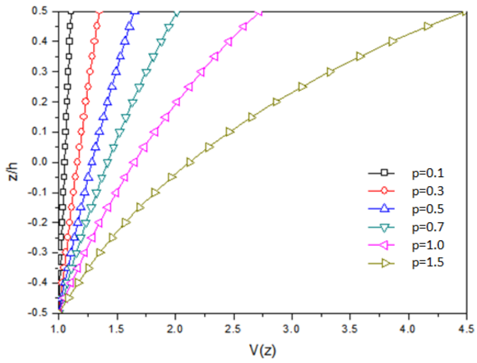

Fig. 2 Exponential function $V(z)$ along the thickness of an EG plate for various values of the parameter p

where E_b denote the property of the bottom surface of the EG plate and p is the parameter that defines the material variation profile along the thickness and takes values greater than zero.

2.2 Kinematic and constitutive relations

The objective of this study is to modify the displacement field with six unknowns of the conventional refined shear deformation plate theory that has been previously proposed by Zenkour (2007), Mantari (2012), Akavci and Tanrikulum (2015) based on some further simplifying assumptions to establish a new kinematics with only five unknowns to predict the static behaviour of the EG plates. It is to be noted that the displacement field of the conventional refined shear deformation theory is given as the form

$$\begin{aligned} u(x,y,z) &= u_0(x,y) - z\frac{\partial w_0}{\partial x} + f(z)\varphi_x(x,y) \\ v(x,y,z) &= v_0(x,y) - z\frac{\partial w_0}{\partial y} + f(z)\varphi_y(x,y) \\ w(x,y,z) &= w_0(x,y) + g(z)\varphi_z(x,y) \end{aligned} \tag{2}$$

where $u_0(x,y), v_0(x,y), w_0(x,y), \varphi_x(x,y), \varphi_y(x,y)$ and $\varphi_z(x,y)$ are the six unknown displacement functions of the mid-plane of the plate and $f(z)$ denote a shape function determining the distribution of the transverse shear strains and the stresses through the thickness of the plate.

By assuming that $\phi_x = \int \theta(x,y)dx$ and $\phi_y = \int \theta(x,y)dy$, the new displacement field of the proposed quasi-3D HySDT is modeled with only five unknowns and can be defined at any material point of the EG plate as follows (Zaoui *et al*. 2018).

$$\begin{aligned} u(x,y,z) &= u_0(x,y) - z\frac{\partial w_0}{\partial x} + k_1 f(z)\int \theta(x,y)dx \\ v(x,y,z) &= v_0(x,y) - z\frac{\partial w_0}{\partial y} + k_2 f(z)\int \theta(x,y)dy \\ w(x,y,z) &= w_0(x,y) + g(z)\varphi_z(x,y) \end{aligned} \tag{3}$$

Here we can note that $\theta\,(x,y)$ is a mathematical term that allows us to obtain the rotations of the normal to the mid-plate about the x and y axes, whereas, the coefficients k_1 and k_2 depends on the geometry of the plate under consideration. Eq. (3) of the proposed theory can be obtained in the case of the 2D analysis by setting $g(z)$=0, however, the shape of the shear function $f(z)$ is chosen to satisfy the free transverse shear stress conditions on the top and bottom surfaces of the plate and is given as Soldatos (1992)

$$f(z) = h\sinh(z/h) - z\cosh(1/2) \tag{4a}$$

and

$$g(z) = \frac{df(z)}{dz} \tag{4b}$$

The strains associated with the displacement field given by Eq. (3) are acquired within the framework of linear theory of elasticity (i.e., Hooke'is law).

$$\begin{Bmatrix} \varepsilon_x \\ \varepsilon_y \\ \gamma_{xy} \end{Bmatrix} = \begin{Bmatrix} \varepsilon_x^0 \\ \varepsilon_y^0 \\ \gamma_{xy}^0 \end{Bmatrix} + z \begin{Bmatrix} \varepsilon_x^1 \\ \varepsilon_y^1 \\ \gamma_{xy}^1 \end{Bmatrix} + f(z) \begin{Bmatrix} \varepsilon_x^2 \\ \varepsilon_y^2 \\ \gamma_{xy}^2 \end{Bmatrix},$$
$$\begin{Bmatrix} \gamma_{yz} \\ \gamma_{xz} \end{Bmatrix} = g(z) \begin{Bmatrix} \gamma_{yz}^0 \\ \gamma_{xz}^0 \end{Bmatrix}, \quad \varepsilon_z = g'(z)\varepsilon_z^0 \tag{5}$$

where

$$\begin{Bmatrix} \varepsilon_x^0 \\ \varepsilon_y^0 \\ \gamma_{xy}^0 \end{Bmatrix} = \begin{Bmatrix} \dfrac{\partial u_0}{\partial x} \\ \dfrac{\partial v_0}{\partial x} \\ \dfrac{\partial u_0}{\partial y} + \dfrac{\partial v_0}{\partial x} \end{Bmatrix}, \quad \begin{Bmatrix} \varepsilon_x^1 \\ \varepsilon_y^1 \\ \gamma_{xy}^1 \end{Bmatrix} = \begin{Bmatrix} -\dfrac{\partial^2 w_0}{\partial x^2} \\ -\dfrac{\partial^2 w_0}{\partial y^2} \\ -2\dfrac{\partial^2 w_0}{\partial x \partial y} \end{Bmatrix},$$
$$\begin{Bmatrix} \varepsilon_x^2 \\ \varepsilon_y^2 \\ \gamma_{xy}^2 \end{Bmatrix} = \begin{Bmatrix} k_1\theta \\ k_2\theta \\ k_1 \dfrac{\partial}{\partial y}\int \theta dx + k_2 \dfrac{\partial}{\partial x}\int \theta dy \end{Bmatrix}, \tag{6a}$$

$$\begin{Bmatrix} \gamma_{yz}^0 \\ \gamma_{xz}^0 \end{Bmatrix} = \begin{Bmatrix} k_2\int \theta dy + \dfrac{\partial \varphi_z}{\partial y} \\ k_1\int \theta dx + \dfrac{\partial \varphi_z}{\partial x} \end{Bmatrix}, \quad \varepsilon_z^0 = \varphi_z \tag{6b}$$

The integrals used in the above relations shall be resolved by a Navier procedure and can be expressed as follows

$$\frac{\partial}{\partial y}\int \theta dx = A'\frac{\partial^2 \theta}{\partial x \partial y}, \quad \frac{\partial}{\partial x}\int \theta dy = B'\frac{\partial^2 \theta}{\partial x \partial y},$$
$$\int \theta dx = A'\frac{\partial \theta}{\partial x}, \quad \int \theta dy = B'\frac{\partial \theta}{\partial y} \tag{7}$$

where A' and B' are determined according to the type of solution employed, in this case via Navier procedure. Thus, the coefficients A',B',k_1 and k_2 are expressed by

$$A' = -\frac{1}{\alpha^2}, \quad B' = -\frac{1}{\beta^2}, \quad k_1 = \alpha^2, \quad k_2 = \beta^2 \tag{8}$$

where the parameters α and β are defined as

$$\alpha = \frac{m\pi}{a}, \quad \beta = \frac{n\pi}{b} \tag{9}$$

The stress-strain relationships accounting for transversal shear deformation in the EG plates coordinates, can be written in matrix forms as

$$\begin{Bmatrix} \sigma_x \\ \sigma_y \\ \sigma_z \end{Bmatrix} = \begin{bmatrix} Q_{11} & Q_{12} & Q_{13} \\ Q_{12} & Q_{22} & Q_{23} \\ Q_{13} & Q_{23} & Q_{33} \end{bmatrix} \begin{Bmatrix} \varepsilon_x \\ \varepsilon_y \\ \varepsilon_z \end{Bmatrix}, \quad \text{and} \quad \begin{Bmatrix} \tau_{yz} \\ \tau_{xz} \\ \tau_{xy} \end{Bmatrix} = \begin{bmatrix} Q_{44} & 0 & 0 \\ 0 & Q_{55} & 0 \\ 0 & 0 & Q_{66} \end{bmatrix} \begin{Bmatrix} \gamma_{yz} \\ \gamma_{xz} \\ \gamma_{xy} \end{Bmatrix} \tag{10}$$

in which $\{\sigma_x, \sigma_y, \sigma_z, \tau_{xy}, \tau_{yz}, \tau_{xz}\}^{Tr}$ and $\{\varepsilon_x, \varepsilon_y, \varepsilon_z, \gamma_{xy}, \gamma_{yz}, \gamma_{xz}\}^{Tr}$ are the stresses and the strains vectors with respect to the plate coordinate system. In the case of the transverse normal strain is different to zero ($\varepsilon_z \neq 0$) the three-dimensional elastic constants Q_{ij} are defined in terms of engineering constants as follows

$$\begin{aligned} Q_{11} &= Q_{22} = Q_{33} = \frac{E(z)(1-\nu)}{(1-2\nu)(1+\nu)}, \\ Q_{12} &= Q_{13} = Q_{23} = \frac{E(z)\nu}{(1-2\nu)(1+\nu)}, \\ Q_{44} &= Q_{55} = Q_{66} = \frac{E(z)}{2(1+\nu)} \end{aligned} \tag{11}$$

Contrarily, in the case of the two-dimensional analysis, the thickness stretching effect is omitted ($\varepsilon_z=0$), so that the material constants Q_{ij} given in Eq. (11) are reduced as

$$\begin{aligned} Q_{11} &= Q_{22} = \frac{E(z)}{(1-\nu^2)}, \quad Q_{12} = \nu\, Q_{11}, \\ Q_{44} &= Q_{55} = Q_{66} = \frac{E(z)}{2(1+\nu)} \end{aligned} \tag{12}$$

2.3 Governing equations

The governing differential equations and boundary conditions of the proposed theory are derived using static version of principle of virtual work for the inhomogeneous plate, where the symbol δ denotes the variational operator. This principle can be stated in the following analytical form (Meksi *et al*. 2019, Draiche *et al*. 2019)

$$\begin{aligned} &\int_{-h/2}^{h/2} \int_A \begin{pmatrix} \sigma_x \delta\varepsilon_x + \sigma_y \delta\varepsilon_y + \sigma_z \delta\varepsilon_z + \\ \tau_{xy}\delta\gamma_{xy} + \tau_{yz}\delta\gamma_{yz} + \tau_{xz}\delta\gamma_{xz} \end{pmatrix} dA dz \\ &- \int_A q\delta w \, dA = 0 \end{aligned} \tag{13}$$

where q is the transverse distributed load applied on the upper surface of the plate. By substituting the expressions for virtual strains given in Eq. (5) into Eq. (13), the principle of virtual work can be rewritten as

$$\int_A \begin{bmatrix} N_x\delta\varepsilon_x^0 + N_y\delta\varepsilon_y^0 + N_z\delta\varepsilon_z^0 + N_{xy}\delta\gamma_{xy}^0 + M_x^b\delta\varepsilon_x^1 \\ +M_y^b\delta\varepsilon_y^1 + M_{xy}^b\delta\gamma_{xy}^1 + M_x^s\delta\varepsilon_x^2 + M_y^s\delta\varepsilon_y^2 \\ +M_{xy}^s\delta\gamma_{xy}^2 + S_{yz}^s\delta\gamma_{yz}^0 + S_{xz}^s\delta\gamma_{xz}^0 - q\delta w \end{bmatrix} dA = 0 \tag{14}$$

where N, M^b, M^s and S^s are the stress resultants defined by the following integrations over the thickness of the plate.

$$\begin{Bmatrix} N_x, & N_y, & N_{xy} \\ M_x^b, & M_y^b, & M_{xy}^b \\ M_x^s, & M_y^s, & M_{xy}^s \end{Bmatrix} = \int_{-h/2}^{h/2} \left(\sigma_x, \sigma_y, \tau_{xy}\right) \begin{Bmatrix} 1 \\ z \\ f(z) \end{Bmatrix} dz,$$

$$N_z = \int_{-h/2}^{h/2} g'(z)\ \sigma_z dz \tag{15a}$$

$$\left(S_{xz}^s, S_{yz}^s\right) = \int_{-h/2}^{h/2} \left(\tau_{xz}, \tau_{yz}\right) g(z)\, dz \tag{15b}$$

Substituting Eq. (5) into stress-strain relations given in Eq. (10) and subsequent results into Eq. (15), the stress resultants of the proposed theory can be obtained in terms of strains according to the following constitutive equations

$$\begin{aligned}
N_x &= A_{11}\varepsilon_x^0 + A_{12}\varepsilon_y^0 + B_{11}\varepsilon_x^1 + B_{12}\varepsilon_y^1 + B_{11}^s\varepsilon_x^2 + B_{12}^s\varepsilon_y^2 + X_{13}\varepsilon_z^0, \\
N_y &= A_{12}\varepsilon_x^0 + A_{22}\varepsilon_y^0 + B_{12}\varepsilon_x^1 + B_{22}\varepsilon_y^1 + B_{12}^s\varepsilon_x^2 + B_{22}^s\varepsilon_y^2 + X_{23}\varepsilon_z^0, \\
N_z &= X_{13}\varepsilon_x^0 + X_{23}\varepsilon_y^0 + Y_{13}\varepsilon_x^1 + Y_{23}\varepsilon_y^1 + Y_{13}^s\varepsilon_x^2 + Y_{23}^s\varepsilon_y^2 + Z_{33}\varepsilon_z^0, \\
N_{xy} &= A_{66}\gamma_{xy}^0 + B_{66}\gamma_{xy}^1 + B_{66}^s\gamma_{xy}^2, \\
M_x^b &= B_{11}\varepsilon_x^0 + B_{12}\varepsilon_y^0 + D_{11}\varepsilon_x^1 + D_{12}\varepsilon_y^1 + D_{11}^s\varepsilon_x^2 + D_{12}^s\varepsilon_y^2 + Y_{13}\varepsilon_z^0, \\
M_y^b &= B_{12}\varepsilon_x^0 + B_{22}\varepsilon_y^0 + D_{12}\varepsilon_x^1 + D_{22}\varepsilon_y^1 + D_{12}^s\varepsilon_x^2 + D_{22}^s\varepsilon_y^2 + Y_{23}\varepsilon_z^0, \\
M_{xy}^b &= B_{66}\gamma_{xy}^0 + D_{66}\gamma_{xy}^1 + D_{66}^s\gamma_{xy}^2, \\
M_x^s &= B_{11}^s\varepsilon_x^0 + B_{12}^s\varepsilon_y^0 + D_{11}^s\varepsilon_x^1 + D_{12}^s\varepsilon_y^1 + H_{11}^s\varepsilon_x^2 + H_{12}^s\varepsilon_y^2 + Y_{13}^s\varepsilon_z^0, \\
M_y^s &= B_{12}^s\varepsilon_x^0 + B_{22}^s\varepsilon_y^0 + D_{12}^s\varepsilon_x^1 + D_{22}^s\varepsilon_y^1 + H_{12}^s\varepsilon_x^2 + H_{22}^s\varepsilon_y^2 + Y_{23}^s\varepsilon_z^0, \\
M_{xy}^s &= B_{66}^s\gamma_{xy}^0 + D_{66}^s\gamma_{xy}^1 + H_{66}^s\gamma_{xy}^2, \quad S_{yz}^s = A_{44}^s\gamma_{yz}^0, \quad S_{xz}^s = A_{55}^s\gamma_{xz}^0
\end{aligned} \tag{16}$$

where A_{ij}, B_{ij}, D_{ij},… *etc*. are the plate stiffness coefficients given by

$$\begin{aligned}
&\left(A_{ij}, B_{ij}, D_{ij}, B_{ij}^s, D_{ij}^s, H_{ij}^s, A_{ij}^s\right) = \\
&\int_{-h/2}^{h/2} Q_{ij}\left(1, z, z^2, f(z), z\,f(z), f^2(z), g^2(z)\right) dz
\end{aligned} \tag{17a}$$

$$\left(X_{ij}, Y_{ij}, Y_{ij}^s, Z_{ij}\right) = \int_{-h/2}^{h/2} g'(z) Q_{ij}\left(1, z, f(z), g'(z)\right) dz \tag{17b}$$

By substituting strains and stresses expressions from Eqs. (6) and (10) into Eq. (14) and integrating by parts and setting the coefficients of δu_0, δv_0, δw_0, $\delta\theta$ and $\delta\varphi_z$ equal to zero, the governing differential equations in terms of stress resultants are obtained as follows

$$
\begin{aligned}
&\delta\ u_0: \quad \frac{\partial N_x}{\partial x}+\frac{\partial N_{xy}}{\partial y}=0\\
&\delta\ v_0: \quad \frac{\partial N_{xy}}{\partial x}+\frac{\partial N_y}{\partial y}=0\\
&\delta\ w_0: \quad \frac{\partial^2 M_x^b}{\partial x^2}+2\frac{\partial^2 M_{xy}^b}{\partial x\partial y}+\frac{\partial^2 M_y^b}{\partial y^2}+q=0\\
&\delta\ \theta: \quad -k_1 M_x^s-k_2 M_y^s-\left(k_1 A'+k_2 B'\right)\frac{\partial^2 M_{xy}^s}{\partial x\partial y}\\
&+k_1 A'\frac{\partial S_{xz}^s}{\partial x}+k_2 B'\frac{\partial S_{yz}^s}{\partial y}=0\\
&\delta\ \phi_z: \quad \frac{\partial S_{xz}^s}{\partial x}+\frac{\partial S_{yz}^s}{\partial y}-N_z=0
\end{aligned} \tag{18}
$$

Using Eqs. (6) and (16), the governing differential equations Eq. (18) based on the present quasi-3D HySDT can be rewritten in terms of displacement variables $(u_0, v_0, w_0, \theta, \varphi_z)$ as

$$
\begin{aligned}
&A_{11}\frac{\partial^2 u_0}{\partial x^2}+A_{66}\frac{\partial^2 u_0}{\partial y^2}+\left(A_{12}+A_{66}\right)\frac{\partial^2 v_0}{\partial x\partial y}-B_{11}\frac{\partial^3 w_0}{\partial x^3}-\left(B_{12}+2B_{66}\right)\frac{\partial^2 w_0}{\partial x\partial y^2}\\
&+\left(k_1 B_{11}^s+k_2 B_{12}^s\right)\frac{\partial\theta}{\partial x}+\left(k_1 A'+k_2 B'\right)B_{66}^s\frac{\partial^3\theta}{\partial x\partial y^2}+X_{13}\frac{\partial\varphi_z}{\partial x}=0
\end{aligned} \tag{19a}
$$

$$
\begin{aligned}
&\left(A_{12}+A_{66}\right)\frac{\partial^2 u_0}{\partial x\partial y}+A_{22}\frac{\partial^2 v_0}{\partial y^2}+A_{66}\frac{\partial^2 v_0}{\partial x^2}-\left(B_{12}+2B_{66}\right)\frac{\partial^3 w_0}{\partial x^2\partial y}-B_{22}\frac{\partial^3 w_0}{\partial y^3}\\
&\left(k_1 B_{12}^s+k_2 B_{22}^s\right)\frac{\partial\theta}{\partial y}+\left(k_1 A'+k_2 B'\right)B_{66}^s\frac{\partial^3\theta}{\partial x^2\partial y}+X_{23}\frac{\partial\varphi_z}{\partial y}=0
\end{aligned} \tag{19b}
$$

$$
\begin{aligned}
&B_{11}\frac{\partial^3 u_0}{\partial x^3}+\left(B_{12}+2B_{66}\right)\frac{\partial^3 u_0}{\partial x\partial y^2}+B_{22}\frac{\partial^3 v_0}{\partial y^3}+\left(B_{12}+2B_{66}\right)\frac{\partial^3 v_0}{\partial x^2\partial y}\\
&-D_{11}\frac{\partial^4 w_0}{\partial x^4}-D_{22}\frac{\partial^4 w_0}{\partial y^4}-2\left(D_{12}+2D_{66}\right)\frac{\partial^4 w_0}{\partial x^2\partial y^2}\\
&+\left(k_1 D_{11}^s+k_2 D_{12}^s\right)\frac{\partial^2\theta}{\partial x^2}+2\left(k_1 A'+k_2 B'\right)D_{66}^s\frac{\partial^4\theta}{\partial x^2\partial y^2}\\
&+\left(k_1 D_{12}^s+k_2 D_{22}^s\right)\frac{\partial^2\theta}{\partial y^2}+Y_{13}\frac{\partial^2\phi_z}{\partial x^2}+Y_{23}\frac{\partial^2\phi_z}{\partial y^2}+q=0
\end{aligned} \tag{19c}
$$

$$
\begin{aligned}
&-\left(k_1 B_{11}^s+k_2 B_{12}^s\right)\frac{\partial u_0}{\partial x}-\left(k_1 B_{12}^s+k_2 B_{22}^s\right)\frac{\partial v_0}{\partial y}\\
&-\left(k_1 A'+k_2 B'\right)B_{66}^s\left(\frac{\partial^3 u_0}{\partial x\partial y^2}+\frac{\partial^3 v_0}{\partial x^2\partial y}\right)\\
&+\left(k_1 D_{11}^s+k_2 D_{12}^s\right)\frac{\partial^2 w_0}{\partial x^2}+2\left(k_1 A'+k_2 B'\right)D_{66}^s\frac{\partial^4 w_0}{\partial x^2\partial y^2}
\end{aligned}
$$

$$
\begin{aligned}
&+\left(k_1 D_{12}^s + k_2 D_{22}^s\right)\frac{\partial^2 w_0}{\partial y^2} - \left(k_1^2 H_{11}^s + k_2^2 H_{22}^s + 2k_1 k_2 H_{12}^s\right)\theta \\
&-\left(k_1 A' + k_2 B'\right)^2 H_{66}^s \frac{\partial^4 \theta}{\partial x^2 \partial y^2} + \left(k_2 B'\right)^2 A_{44}^s \frac{\partial^2 \theta}{\partial y^2} \\
&+\left(k_1 A'\right)^2 A_{55}^s \frac{\partial^2 \theta}{\partial x^2} + k_1 A' A_{55}^s \frac{\partial^2 \phi_z}{\partial x^2} + k_2 B' A_{44}^s \frac{\partial^2 \phi_z}{\partial y^2} \\
&-\left(k_1 Y_{13}^s + k_2 Y_{23}^s\right)\phi_z = 0
\end{aligned}
\tag{19d}
$$

$$
\begin{aligned}
&-X_{13}\frac{\partial u_0}{\partial x} - X_{23}\frac{\partial v_0}{\partial y} + Y_{13}^s \frac{\partial^2 w_0}{\partial x^2} + Y_{23}^s \frac{\partial^2 w_0}{\partial y^2} - \left(k_1 Y_{13}^s + k_2 Y_{23}^s\right)\theta \\
&+k_1 A' A_{55}^s \frac{\partial^2 \theta}{\partial x^2} + k_2 B' A_{44}^s \frac{\partial^2 \theta}{\partial y^2} + A_{55}^s \frac{\partial^2 \varphi_z}{\partial x^2} + A_{44}^s \frac{\partial^2 \varphi_z}{\partial y^2} - Z_{33}\varphi_z = 0
\end{aligned}
\tag{19e}
$$

2.4 Analytical solution procedure for EG Plates

In this study, the analytical solutions of Eq. (19) for simply supported EG plates under transverse mechanical load can be obtained, by considering the Navier'is solution procedure, the following expressions of displacement variables are represented in the double trigonometric series, which satisfy governing differential equations and boundary conditions exactly (Balubaid *et al.* 2019, Abualnour *et al.* 2019, Adda Bedia *et al.* 2019, Karami *et al.* 2019c).

$$
\begin{Bmatrix} u_0 \\ v_0 \\ w_0 \\ \theta \\ \varphi_z \end{Bmatrix} = \sum_{m=1}^{\infty}\sum_{n=1}^{\infty} \begin{Bmatrix} U_{mn}\cos(\alpha\, x)\sin(\beta\, y) \\ V_{mn}\sin(\alpha\, x)\cos(\beta\, y) \\ W_{mn}\sin(\alpha\, x)\sin(\beta\, y) \\ \Theta_{mn}\sin(\alpha\, x)\sin(\beta\, y) \\ \Phi_{mn}\sin(\alpha\, x)\sin(\beta\, y) \end{Bmatrix}
\tag{20}
$$

where U_{mn}, V_{mn}, W_{mn}, Θ_{mn} and Φ_{mn} are unknown coefficients, so the parameters α and β are already defined in Eq. (9). The transverse load $q(x,y)$ acting on the top surface of the plate is also expanded in double-Fourier sine series as

$$
q(x,y) = \sum_{m=1}^{\infty}\sum_{n=1}^{\infty} Q_{mn}\sin(\alpha\, x)\cos(\beta\, y)
\tag{21}
$$

where the coefficient Q_{mn}=q_0 for sinusoidal distributed load m=2, n=1. Whereas, q_0 is the maximum intensity of distributed load at the centre of plate. Substitution of this solution of Eq. (20) into the governing equations Eq. (19), the analytical solutions of EG plates can be obtained from the following matrix form

$$
\begin{bmatrix} k_{11} & k_{12} & k_{13} & k_{14} & k_{15} \\ k_{12} & k_{22} & k_{23} & k_{24} & k_{25} \\ k_{13} & k_{23} & k_{33} & k_{34} & k_{35} \\ k_{14} & k_{24} & k_{34} & k_{44} & k_{45} \\ k_{15} & k_{25} & k_{35} & k_{45} & k_{55} \end{bmatrix}
\begin{Bmatrix} U_{mn} \\ V_{mn} \\ W_{mn} \\ \Theta_{mn} \\ \Phi_{mn} \end{Bmatrix} = \begin{Bmatrix} 0 \\ 0 \\ Q_{mn} \\ 0 \\ 0 \end{Bmatrix}
\tag{22}
$$

Table 1 Non-dimensional transverse displacement $\overline{w}$ (a/2, b/2, 0) for various EG plates, a/h=2

b/a	Theory	ε_z	p					
			0.1	0.3	0.5	0.7	1.0	1.5
6	3-D (Zenkour 2007)	≠0	1.63774	1.48846	1.35184	1.22688	1.05929	0.82606
	Present	≠0	1.63665	1.47963	1.33654	1.20627	1.03268	0.79388
	Present	=0	1.73471	1.56890	1.41828	1.28151	1.09968	0.84997
	Mantari and Soares(2013)	≠0	1.63654	1.47953	1.33644	1.20618	1.03325	0.79387
	Mantari and Soares(2012)	=0	1.73465	1.56884	1.41822	1.28145	1.10032	0.84996
	TPT(Zenkour2007)	≠0	1.62939	1.47309	1.33066	1.20101	1.02823	0.79056
	HPT (Zenkour 2007)	=0	1.54777	1.39964	1.26493	1.14249	0.97956	0.75560
5	3-D (Zenkour 2007)	≠0	1.60646	1.46007	1.32607	1.20349	1.03907	0.81024
	Present	≠0	1.60543	1.45141	1.31104	1.18325	1.01295	0.77868
	Present	=0	1.70252	1.53978	1.39193	1.25767	1.07918	0.83402
	Mantari and Soares (2013)	≠0	1.60532	1.45130	1.31094	1.18315	1.01352	0.77867
	Mantari and Soares (2012)	=0	1.70246	1.53972	1.39188	1.25762	1.07981	0.83401
	TPT (Zenkour 2007)	≠0	1.59825	1.44493	1.30522	1.17804	1.00856	0.77540
	HPT (Zenkour 2007)	=0	1.51991	1.37444	1.24214	1.12188	0.96184	0.74184
4	3-D (Zenkour 2007)	≠0	1.55146	1.41013	1.28074	1.16235	1.00352	0.78241
	Present	≠0	1.55053	1.40177	1.26619	1.14276	0.97827	0.75196
	Present	=0	1.64590	1.48855	1.34558	1.21574	1.04310	0.80597
	Mantari and Soares (2013)	≠0	1.55042	1.40166	1.26610	1.14267	0.97884	0.75195
	Mantari and Soares (2012)	=0	1.64584	1.48849	1.34553	1.21569	1.04374	0.80596
	TPT (Zenkour 2007)	≠0	1.54348	1.39541	1.26048	1.13764	0.97395	0.74874
	HPT (Zenkour 2007)	=0	1.47089	1.33009	1.20201	1.08559	0.93065	0.71762
3	3-D (Zenkour 2007)	≠0	1.44295	1.31160	1.19129	1.08117	0.93337	0.72750
	Present	≠0	1.44221	1.30383	1.17771	1.06288	0.90984	0.69926
	Present	=0	1.53411	1.38740	1.25407	1.13296	0.97190	0.75061
	Mantari and Soares (2013)	≠0	1.44210	1.30373	1.17761	1.06279	0.91041	0.69925
	Mantari and Soares (2012)	=0	1.53405	1.38735	1.25402	1.13291	0.97254	0.7506
	TPT (Zenkour 2007)	≠0	1.43542	1.29771	1.17221	1.05795	0.90567	0.69615
	HPT (Zenkour 2007)	=0	1.37394	1.24238	1.12269	1.01386	0.86898	0.66977
2	3-D (Zenkour 2007)	≠0	1.19445	1.08593	0.98640	0.89520	0.77266	0.60174
	Present	≠0	1.19419	1.07959	0.97513	0.87999	0.75318	0.57864
	Present	=0	1.27766	1.15539	1.04419	0.94312	0.80864	0.62378
	Mantari and Soares (2013)	≠0	1.19408	1.07949	0.97503	0.87990	0.75377	0.57862
	Mantari and Soares (2012)	=0	1.27760	1.15533	1.04413	0.94307	0.80929	0.62377
	TPT (Zenkour 2007)	≠0	1.18798	1.07399	0.97009	0.87548	0.74936	0.57578
	HPT (Zenkour 2007)	=0	1.15080	1.04052	0.94012	0.84878	0.72712	0.55975
1	3-D (Zenkour 2007)	≠0	0.57693	0.52473	0.47664	0.43240	0.37269	0.28904
	Present	≠0	0.57800	0.52251	0.47189	0.42577	0.36423	0.27942
	Present	=0	0.63631	0.57523	0.51953	0.46879	0.40113	0.30792
	Mantari and Soares (2013)	≠0	0.57789	0.52240	0.47179	0.42567	0.36485	0.27939
	Mantari and Soares (2012)	=0	0.63625	0.57517	0.51948	0.46874	0.40178	0.30791
	TPT (Zenkour 2007)	≠0	0.57308	0.51806	0.46788	0.42216	0.36117	0.27712
	HPT (Zenkour 2007)	=0	0.58586	0.52955	0.47814	0.43127	0.36871	0.28246

where the elements of stiffness matrix [K] are obtained as follows

$$
\begin{aligned}
&k_{11}=\alpha^2 A_{11}+\beta^2 A_{66},\ k_{12}=\alpha\beta\, A_{12}+\alpha\beta A_{66},\\
&k_{13}=-\alpha^3 B_{11}-\alpha\beta^2 B_{12}-2\alpha\beta^2 B_{66},\\
&k_{14}=-k_1\alpha B_{11}^s-k_2\alpha B_{12}^s+\left(k_1 A'+k_2 B'\right)\alpha\beta^2 B_{66}^s,\\
&k_{15}=-\alpha X_{13}, k_{22}=\beta^2 A_{22}+\alpha^2 A_{66},\\
&k_{23}=-\beta^3 B_{22}-\alpha^2\beta B_{12}-2\alpha^2\beta B_{66},\\
&k_{24}=-k_1\beta B_{12}^s-k_2\beta B_{22}^s+\left(k_1 A'+k_2 B'\right)\alpha^2\beta B_{66}^s,\\
&k_{25}=-\beta X_{23},\\
&k_{33}=\alpha^4 D_{11}+2\alpha^2\beta^2 D_{12}+\beta^4 D_{22}+4\alpha^2\beta^2 D_{66},\\
&k_{34}=k_1\left(\alpha^2 D_{11}^s+\beta^2 D_{12}^s\right)+k_2\left(\alpha^2 D_{12}^s+\beta^2 D_{22}^s\right)-\\
&2\left(k_1 A'+k_2 B'\right)\alpha^2\beta^2 D_{66}^s,\ k_{35}=\alpha^2 Y_{13}+\beta^2 Y_{23},\\
&k_{44}=-\left(k_1 A'+k_2 B'\right)^2\alpha^2\beta^2 H_{66}^s+k_1\left(k_1 H_{11}^s+k_2 H_{12}^s\right)\\
&+k_2\left(k_1 H_{12}^s+k_2 H_{22}^s\right)+\left(k_2 B'\right)^2\beta^2 A_{44}^s+\left(k_1 A'\right)^2\alpha^2 A_{55}^s,\\
&k_{45}=k_1 Y_{13}^s+k_2 Y_{23}^s+k_2 B'\beta^2 A_{44}^s+k_1 A'\alpha^2 A_{55}^s,\\
&k_{55}=\beta^2 A_{44}^s+\alpha^2 A_{55}^s+Z_{33}
\end{aligned}
\tag{23}
$$

4. Numerical results and discussions

In this section, the functionally graded material plates made of aluminum as metal (bottom surface) graded exponentially trough the thickness of a rectangular plate are provided and used to investigate the static behaviour of simply supported EG plates at all edges and subjected to sinusoidal distributed load, by using the simple and accurate hyperbolic quasi-3D and 2D higher-order shear deformation theories. The non-dimensional displacements and stresses are presented and compared with the corresponding results of various 2D and quasi-3D shear deformation theories available in literature and the exact elasticity solution given by Zenkour (2007) wherever applicable. The material properties used for calculating the numerical results are

$$E_b=70\,GPa,\quad \nu_b=0.3 \tag{24}$$

For the simplicity, the following non-dimensional terms given here are employed to normalize displacements and stresses

$$
\begin{aligned}
&\bar{u}\left(0,\frac{b}{2},z\right)=\frac{10h^3E_b}{qa^4}u,\quad \bar{v}\left(\frac{a}{2},0,z\right)=\frac{10h^3E_b}{qa^4}v,\quad \bar{w}\left(\frac{a}{2},\frac{b}{2},z\right)=\frac{10h^3E_b}{qa^4}w,\\
&\bar{\sigma}_x\left(\frac{a}{2},\frac{b}{2},z\right)=\frac{h^2}{qa^2}\sigma_x,\quad \bar{\sigma}_y\left(\frac{a}{2},\frac{b}{2},z\right)=\frac{h^2}{qa^2}\sigma_y,\quad \bar{\tau}_{xy}(0,0,z)=\frac{h^2}{qa^2}\tau_{xy},\\
&\bar{\tau}_{xz}\left(0,\frac{b}{2},z\right)=\frac{h}{qa}\tau_{xz},\quad \bar{\tau}_{yz}\left(\frac{a}{2},0,z\right)=\frac{h}{qa}\tau_{yz}
\end{aligned}
\tag{25}
$$

Table 2 Non-dimensional transverse displacement $\overline{w}$ (a/2, b/2, 0) for various EG plates, a/h=4

b/a	Theory	ε_z	p					
			0.1	0.3	0.5	0.7	1.0	1.5
6	3-D (Zenkour 2007)	≠0	1.17140	1.06218	0.96331	0.87378	0.75501	0.59193
	Present	≠0	1.17033	1.05825	0.95628	0.86359	0.74033	0.57129
	Present	=0	1.19202	1.07886	0.97668	0.88437	0.76229	0.59545
	Mantari and Soares (2013)	≠0	1.17033	1.05825	0.95628	0.86359	0.74032	0.57128
	Mantari and Soares (2012)	=0	1.19202	1.07885	0.97667	0.88437	0.76228	0.59545
	TPT (Zenkour 2007)	≠0	1.16681	1.05509	0.95345	0.86107	0.73821	0.56969
	HPT (Zenkour 2007)	=0	1.00649	0.91087	0.82448	0.74640	0.64306	0.50178
5	3-D (Zenkour 2007)	≠0	1.14589	1.03906	0.94236	0.85478	0.73859	0.57904
	Present	≠0	1.14484	1.03520	0.93545	0.84478	0.72419	0.55883
	Present	=0	1.16628	1.05556	0.95558	0.86526	0.74579	0.58253
	Mantari and Soares (2013)	≠0	1.14484	1.03520	0.93545	0.84478	0.72419	0.55882
	Mantari and Soares (2012)	=0	1.16628	1.05555	0.95557	0.86525	0.74578	0.58253
	TPT (Zenkour 2007)	≠0	1.14140	1.03210	0.93268	0.84231	0.72212	0.55726
	HPT (Zenkour 2007)	=0	0.98508	0.89150	0.80694	0.73050	0.62935	0.49105
4	3-D (Zenkour 2007)	≠0	1.10115	0.99852	0.90560	0.82145	0.70979	0.55643
	Present	≠0	1.10013	0.99477	0.89891	0.81178	0.69589	0.53697
	Present	=0	1.12114	1.01469	0.91857	0.83173	0.71686	0.55987
	Mantari and Soares (2013)	≠0	1.10013	0.99477	0.89891	0.81178	0.69589	0.53696
	Mantari and Soares (2012)	=0	1.12113	1.01469	0.91856	0.83172	0.71685	0.55987
	TPT (Zenkour 2007)	≠0	1.09682	0.99180	0.89625	0.80941	0.69390	0.53546
	HPT (Zenkour 2007)	=0	0.94753	0.85750	0.77615	0.70262	0.60529	0.47222
3	3-D (Zenkour 2007)	≠0	1.01338	0.91899	0.83350	0.75606	0.65329	0.51209
	Present	≠0	1.01243	0.91546	0.82724	0.74704	0.64037	0.49409
	Present	=0	1.03255	0.93450	0.84595	0.76593	0.66008	0.51541
	Mantari and Soares (2013)	≠0	1.01243	0.91546	0.82724	0.74704	0.64037	0.49408
	Mantari and Soares (2012)	=0	1.03254	0.93450	0.84594	0.76593	0.66008	0.51541
	TPT (Zenkour 2007)	≠0	1.00938	0.91272	0.82479	0.74486	0.63854	0.49270
	HPT (Zenkour 2007)	=0	0.87379	0.79076	0.71571	0.64787	0.55806	0.43525
2	3-D (Zenkour 2007)	≠0	0.81529	0.73946	0.67075	0.60846	0.52574	0.41200
	Present	≠0	0.81448	0.73647	0.66547	0.60094	0.51509	0.39732
	Present	=0	0.83246	0.75338	0.68193	0.61735	0.53188	0.41504
	Mantari and Soares (2013)	≠0	0.81448	0.73647	0.66547	0.60093	0.51508	0.39732
	Mantari and Soares (2012)	=0	0.83246	0.75338	0.68192	0.61734	0.53188	0.41503
	TPT (Zenkour 2007)	≠0	0.81202	0.73425	0.66350	0.59917	0.51361	0.39620
	HPT (Zenkour 2007)	=0	0.70700	0.63979	0.57901	0.52405	0.45126	0.35169
1	3-D (Zenkour 2007)	≠0	0.34900	0.31677	0.28747	0.26083	0.22534	0.18054
	Present	≠0	0.34860	0.31519	0.28477	0.25711	0.22028	0.16973
	Present	=0	0.36017	0.32589	0.29485	0.26676	0.22953	0.17854
	Mantari and Soares (2013)	≠0	0.34860	0.31519	0.28477	0.25710	0.22028	0.16972
	Mantari and Soares (2012)	=0	0.36017	0.32589	0.29485	0.26676	0.22952	0.17854
	TPT (Zenkour 2007)	≠0	0.34749	0.31419	0.28388	0.25631	0.21961	0.16922
	HPT (Zenkour 2007)	=0	0.31111	0.28146	0.25461	0.23027	0.19800	0.15377

The transverse displacements, normal stresses, and shears stresses through the thickness of EG plates defined by Eq. (25) in non-dimensional form are presented in Tables 1 to 8 for different values of side-to-thickness ratio (*a/h*=2, 4, 10), aspect ratio (*b/a*=1, 2, 3, 4, 5, 6) and material parameter values *p*. The graphical results obtained by using the present hyperbolic plate theory with five unknowns, which include the stretching effect ($\varepsilon_z \neq 0$) and the previous studies such as Guedes Soares (2013) and Zenkour (2007) based on a quasi-3D trigonometric plate theory (TPT) with six unknowns are also plotted in Figs. 3 to 9.

Tables 1-3 present the transverse maximum displacements of geometrically different EG plates. The obtained results are compared with 3-D elasticity solution, 2D higher-order plate theory (HPT) and quasi-3D trigonometric plate theory (TPT) reported by Zenkour (2007) and 2D and quasi-3D trigonometric plate theories, which includes tangential function developed by Mantari and Guedes

Table 3 Non-dimensional transverse displacement $\overline{w}$ (*a/2*, *b/2*, 0) for various EG plates, *a/h = 10*

b/a	Theory	ε_z	*p* 0.1	0.3	0.5	0.7	1.0	1.5	2.0	2.5	3.0
6	Present	≠0	1.0354	0.9363	0.8462	0.7644	0.6558	0.5069	0.3913	0.3018	0.2324
	Present	=0	1.0388	0.9405	0.8520	0.7723	0.6670	0.5236	0.4115	0.3235	0.2539
	Mantari and Soares (2013)	≠0	1.0354	0.9363	0.8462	0.7644	0.6558	0.5069	0.3913	0.3018	0.2324
	Mantari and Soares (2012)	=0	1.0388	0.9405	0.8520	0.7723	0.6670	0.5236	0.4115	0.3235	0.2539
	TPT (Mantari and Soares 2013)	≠0	1.0321	0.9333	0.8436	0.7621	0.6538	0.5054	0.3901	0.3006	0.2314
5	Present	≠0	1.0115	0.9147	0.8267	0.7468	0.6406	0.4952	0.3823	0.2948	0.2271
	Present	=0	1.0149	0.9189	0.8324	0.7545	0.6516	0.5115	0.4020	0.3160	0.2480
	Mantari and Soares (2013)	≠0	1.0115	0.9147	0.8267	0.7468	0.6406	0.4952	0.3823	0.2948	0.2271
	Mantari and Soares (2012)	=0	1.0149	0.9189	0.8324	0.7545	0.6516	0.5115	0.4020	0.3160	0.2480
	TPT (Mantari and Soares 2013)	≠0	1.0083	0.9118	0.8241	0.7445	0.6387	0.4938	0.3810	0.2937	0.2261
4	Present	≠0	0.9696	0.8768	0.7925	0.7159	0.6141	0.4747	0.3664	0.2826	0.2177
	Present	=0	0.9730	0.8809	0.7980	0.7233	0.6247	0.4903	0.3854	0.3029	0.2377
	Mantari and Soares (2013)	≠0	0.9696	0.8768	0.7925	0.7159	0.6141	0.4747	0.3664	0.2826	0.2177
	Mantari and Soares (2012)	=0	0.9730	0.8809	0.7980	0.7233	0.6247	0.4903	0.3854	0.3029	0.2377
	TPT (Mantari and Soares 2013)	≠0	0.9665	0.8741	0.7900	0.7137	0.6123	0.4733	0.3653	0.2815	0.2167
3	Present	≠0	0.8877	0.8027	0.7255	0.6554	0.5622	0.4346	0.3355	0.2587	0.1992
	Present	=0	0.8909	0.8066	0.7307	0.6622	0.5720	0.4489	0.3528	0.2773	0.2176
	Mantari and Soares (2013)	≠0	0.8877	0.8027	0.7255	0.6554	0.5622	0.4346	0.3355	0.2587	0.1992
	Mantari and Soares (2012)	=0	0.8909	0.8066	0.7307	0.6622	0.5720	0.4489	0.3528	0.2773	0.2176
	TPT (Mantari and Soares 2013)	≠0	0.8849	0.8002	0.7233	0.6534	0.5605	0.4333	0.3344	0.2577	0.1983

Table 3 Continued

b/a	Theory	ε_z	*p* 0.1	0.3	0.5	0.7	1.0	1.5	2.0	2.5	3.0
2	Present	≠0	0.7037	0.6364	0.5752	0.5196	0.4457	0.3445	0.2659	0.2050	0.1579
	Present	=0	0.7066	0.6397	0.5795	0.5252	0.4536	0.3560	0.2797	0.2198	0.1724
	Mantari and Soares (2013)	≠0	0.7037	0.6364	0.5752	0.5196	0.4457	0.3445	0.2659	0.2050	0.1579
	Mantari and Soares (2012)	=0	0.7066	0.6397	0.5795	0.5252	0.4536	0.3560	0.2797	0.2198	0.1724
	TPT (Mantari and Soares 2013)	≠0	0.7015	0.6344	0.5734	0.5180	0.4444	0.3435	0.2651	0.2043	0.1572
1	Present	≠0	0.2799	0.2531	0.2287	0.2066	0.1772	0.1370	0.1057	0.0814	0.0627
	Present	=0	0.2816	0.2550	0.2309	0.2093	0.1807	0.1417	0.1112	0.0873	0.0684
	Mantari and Soares (2013)	≠0	0.2799	0.2531	0.2287	0.2066	0.1772	0.1370	0.1057	0.0814	0.0627
	Mantari and Soares (2012)	=0	0.2816	0.2550	0.2309	0.2093	0.1807	0.1417	0.1112	0.0873	0.0684
	TPT (Mantari and Soares 2013)	≠0	0.2790	0.2523	0.2280	0.2060	0.1767	0.1366	0.1053	0.0811	0.0624

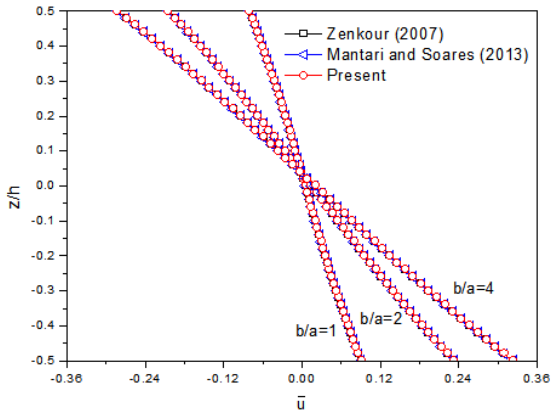

Fig. 3 Distribution of non-dimensional axial displacement $(\bar{u})$, through the thickness of a thick EG plate (*a/h*=4, *p*=0.5)

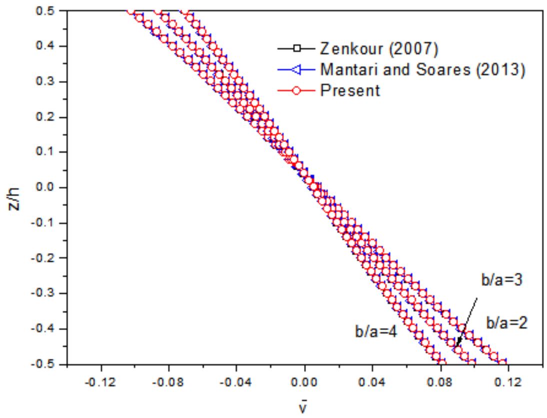

Fig. 4 Distribution of non-dimensional axial displacement $(\bar{v})$, through the thickness of a thick EG plate (*a/h*=4, *p*=0.5)

Soares (2012, 2013). It can be observed that the numerical results obtained by using the present 2D hyperbolic shear deformation plate theory (HySDT) are in excellent agreement with the 2D HSDT results of Mantari and Guedes Soares (2012). In addition, the present quasi-3D HySDT and quasi-3D HSDT of Mantari and Guedes Soares (2013) are in good agreement with each other for all aspect ratio and material parameter values ranging from very thick to moderately thick EG plates.

Moreover, it can be seen that the results are much closer to the exact elasticity solutions in the case where the stretching effect is considered. However, 2D theories which do not include the thickness stretching effect overestimate the results for the different models proposed due to neglect of transverse normal deformation. It should be noted that the results for the non-dimensional

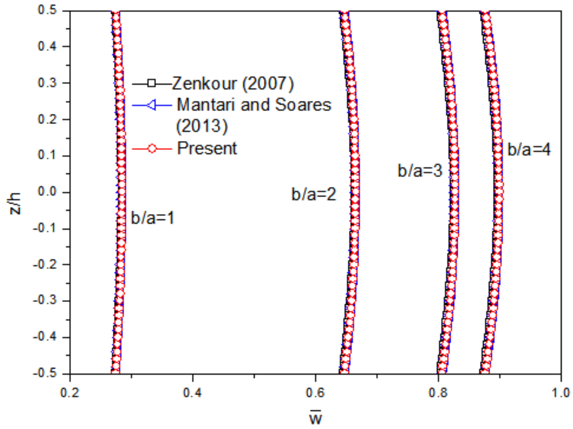

Fig. 5 Distribution of non-dimensional transverse displacement $(\overline{w})$, through the thickness of a thick EG plate (*a/h*=4, *p*=0.5)

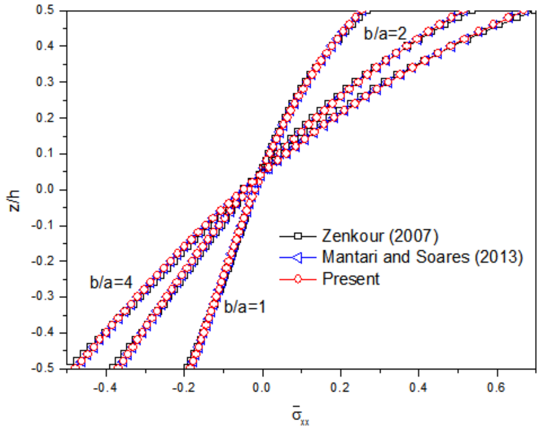

Fig. 6 Distribution of non-dimensional axial stress $(\overline{\sigma}_{xx})$, through the thickness of a thick EG plate (*a/h*=4, *p*=0.5)

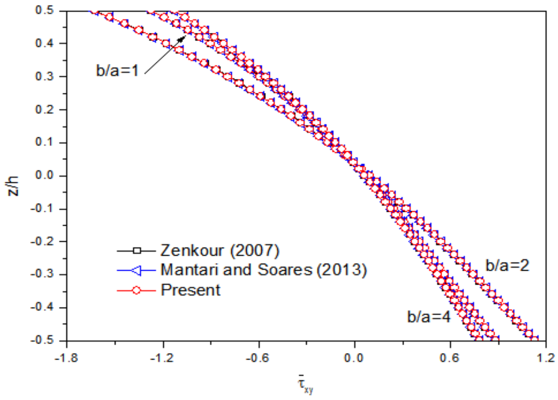

Fig. 7 Distribution of non-dimensional inplane shear stress $(\overline{\tau}_{xy})$, through the thickness of a thick EG plate (*a/h*=4, *p*=0.5)

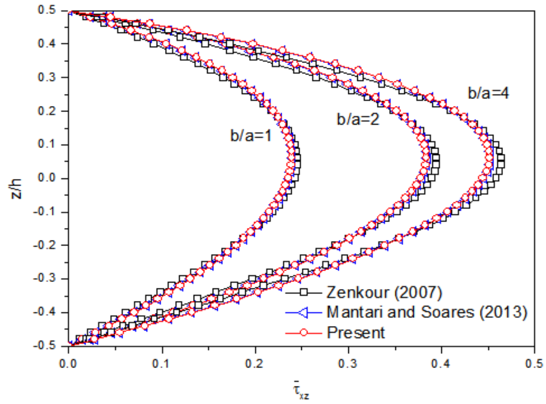

Fig. 8 Distribution of non-dimensional transverse shear stress $(\overline{\tau}_{xz})$, through the thickness of a thick EG plate (*a/h*=4, *p*=0.5)

transverse displacements increase with the decrease of the parameter *p* and the increase of the aspect ratio *a/b*, it is clearly that this is due to the reduction in the stiffness of the plate.

Figs. 3-9 illustrate the axial and transverse displacements $\overline{u}, \overline{v}, \overline{w}$ and stresses $(\overline{\sigma}_x, \overline{\tau}_{xy}, \overline{\tau}_{xz}, \overline{\tau}_{yz})$ distributions through the thickness of thick EG plates for the thickness ratio (*a/h*=4) and the material parameter (*p*=0.5) calculated using constitutive relations as well as by the governing equations of the present quasi-3D HySDT and quasi-3D TPT with six unknowns developed by Zenkour (2007) and with the quasi-3D HSDT generated by Mantari and Guedes Soares (2013) based on another form of the displacement field in which the tangential trigonometric function is included. Examination of these figures reveals that the present theory produces good results compared with each other.

The comparison of the non-dimensional axial normal stress for simply supported rectangular EG plates under sinusoidal distributed load is reported in Tables 4-6 for three values of the thickness

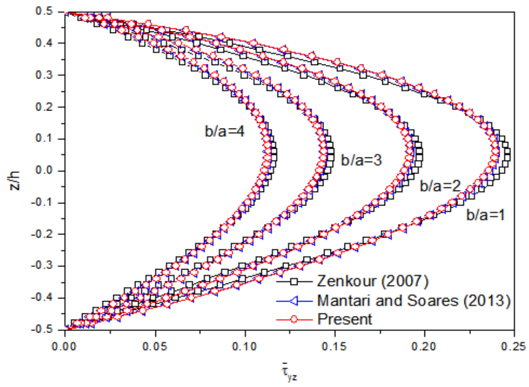

Fig. 9 Distribution of non-dimensional transverse shear stress $(\bar{\tau}_{yz})$, through the thickness of a thick EG plate (*a/h*=4, *p*=0.5)

Table 4 Non-dimensional axial stress $\bar{\sigma}_{yy}$ (*a*/2, *b*/2, *h*/2) for various EG plates, *a/h*=2

b/a	Theory	ε_z	*p*					
			0.1	0.3	0.5	0.7	1.0	1.5
6	3-D (Zenkour 2007)	≠0	0.29429	0.31008	0.32699	0.34508	0.37456	0.43051
	Present	≠0	0.27593	0.29507	0.31551	0.33736	0.37301	0.44107
	Present	=0	0.21862	0.23437	0.25111	0.26898	0.29763	0.35164
	Mantari and Soares (2013)	≠0	0.27628	0.29544	0.31592	0.33780	0.37374	0.44163
	Mantari and Soares (2012)	=0	0.21871	0.23447	0.25122	0.26900	0.29804	0.34981
	TPT (Zenkour 2007)	≠0	0.29119	0.31184	0.33385	0.35731	0.39547	0.46786
	HPT (Zenkour 2007)	=0	0.31192	0.33462	0.35873	0.38433	0.42573	0.50345
5	3-D (Zenkour 2007)	≠0	0.29674	0.31277	0.32993	0.34829	0.37821	0.43500
	Present	≠0	0.27859	0.29796	0.31865	0.34076	0.37683	0.44559
	Present	=0	0.22175	0.23774	0.25472	0.27276	0.30194	0.35675
	Mantari and Soares (2013)	≠0	0.27892	0.29833	0.31905	0.34119	0.37755	0.44614
	Mantari and Soares (2012)	=0	0.22185	0.23784	0.25484	0.27288	0.30236	0.35485
	TPT (Zenkour 2007)	≠0	0.29353	0.31439	0.33662	0.36032	0.39884	0.47187
	HPT (Zenkour 2007)	=0	0.31327	0.33607	0.36030	0.38604	0.42764	0.50573
4	3-D (Zenkour 2007)	≠0	0.30084	0.31727	0.33486	0.35368	0.38435	0.44257
	Present	≠0	0.28303	0.30281	0.32393	0.34648	0.38323	0.45320
	Present	=0	0.22705	0.24344	0.26084	0.27933	0.30923	0.36539
	Mantari and Soares (2013)	≠0	0.28335	0.30317	0.32431	0.34690	0.38394	0.45373
	Mantari and Soares (2012)	=0	0.22715	0.24354	0.26096	0.27945	0.30968	0.36337
	TPT (Zenkour 2007)	≠0	0.29743	0.31864	0.34124	0.36533	0.40446	0.47857
	HPT (Zenkour 2007)	=0	0.31543	0.33842	0.36285	0.38878	0.43072	0.50943
3	3-D (Zenkour 2007)	≠0	0.30808	0.32525	0.34362	0.36329	0.39534	0.45619
	Present	≠0	0.29092	0.31144	0.33333	0.35668	0.39468	0.46682
	Present	=0	0.23665	0.25376	0.27194	0.29124	0.32246	0.38111
	Mantari and Soares (2013)	≠0	0.29122	0.31177	0.33369	0.35707	0.39537	0.46732
	Mantari and Soares (2012)	=0	0.23675	0.25387	0.27206	0.29138	0.32297	0.37881
	TPT (Zenkour 2007)	≠0	0.30421	0.32606	0.34933	0.37410	0.41432	0.49035
	HPT (Zenkour 2007)	=0	0.31890	0.34220	0.36695	0.39323	0.43572	0.51545

Table 4 Continued

b/a	Theory	ε_z	p					
			0.1	0.3	0.5	0.7	1.0	1.5
2	3-D (Zenkour 2007)	≠0	0.31998	0.33849	0.35833	0.37956	0.41417	0.47989
	Present	≠0	0.30398	0.32586	0.34916	0.37395	0.41418	0.49012
	Present	=0	0.25373	0.27218	0.29178	0.31259	0.34625	0.40943
	Mantari and Soares (2013)	≠0	0.30422	0.32613	0.34945	0.37427	0.41483	0.49052
	Mantari and Soares (2012)	=0	0.25385	0.27231	0.29193	0.31276	0.34690	0.40636
	TPT (Zenkour 2007)	≠0	0.31463	0.33758	0.36200	0.38796	0.43003	0.50925
	HPT (Zenkour 2007)	=0	0.32223	0.34592	0.37109	0.39782	0.44102	0.52203
1	3-D (Zenkour 2007)	≠0	0.31032	0.32923	0.34953	0.37127	0.40675	0.47405
	Present	≠0	0.29237	0.31460	0.33817	0.36316	0.40339	0.47835
	Present	=0	0.25198	0.27081	0.29081	0.31204	0.34634	0.41056
	Mantari and Soares (2013)	≠0	0.29244	0.31468	0.33826	0.36325	0.40405	0.47848
	Mantari and Soares (2012)	=0	0.25215	0.27100	0.29102	0.31227	0.34773	0.40347
	TPT (Zenkour 2007)	≠0	0.29554	0.31811	0.34208	0.36750	0.40851	0.48508
	HPT (Zenkour 2007)	=0	0.28882	0.31072	0.33398	0.35866	0.39852	0.47305

Table 5 Non-dimensional axial stress $\bar{\sigma}_{yy}$ ($a/2$, $b/2$, $h/2$) for various EG plates, a/h=4

b/a	Theory	ε_z	p					
			0.1	0.3	0.5	0.7	1.0	1.5
6	3-D (Zenkour 2007)	≠0	0.21814	0.23211	0.24699	0.26284	0.28857	0.33725
	Present	≠0	0.21210	0.22487	0.23869	0.25370	0.27875	0.32847
	Present	=0	0.20096	0.21492	0.22975	0.24552	0.27104	0.31915
	Mantari and Soares (2013)	≠0	0.21265	0.22547	0.23934	0.2544	0.27953	0.32937
	Mantari and Soares (2012)	=0	0.20097	0.21493	0.22976	0.24553	0.27105	0.31917
	TPT (Zenkour 2007)	≠0	0.23686	0.25204	0.26830	0.28574	0.31441	0.36990
	HPT (Zenkour 2007)	=0	0.28170	0.30133	0.32219	0.34435	0.38024	0.44786
5	3-D (Zenkour 2007)	≠0	0.22060	0.23476	0.24984	0.26591	0.29199	0.34133
	Present	≠0	0.21470	0.22771	0.24177	0.25702	0.28246	0.33284
	Present	=0	0.20365	0.21780	0.23284	0.24881	0.27468	0.32345
	Mantari and Soares (2013)	≠0	0.21524	0.2283	0.24241	0.25772	0.28323	0.33373
	Mantari and Soares (2012)	=0	0.20366	0.21781	0.23285	0.24883	0.27470	0.32346
	TPT (Zenkour 2007)	≠0	0.23912	0.25450	0.27097	0.28863	0.31764	0.37371
	HPT (Zenkour 2007)	=0	0.28261	0.30231	0.32323	0.34547	0.38148	0.44934
4	3-D (Zenkour 2007)	≠0	0.22470	0.23918	0.25460	0.27103	0.29770	0.34816
	Present	≠0	0.21904	0.23244	0.24691	0.26259	0.28868	0.34018
	Present	=0	0.20817	0.22263	0.23801	0.25434	0.28079	0.33065
	Mantari and Soares (2013)	≠0	0.21957	0.23302	0.24754	0.26327	0.28943	0.34105
	Mantari and Soares (2012)	=0	0.20818	0.22264	0.23802	0.25435	0.28081	0.33066
	TPT (Zenkour 2007)	≠0	0.24286	0.25858	0.27539	0.29342	0.32299	0.38004
	HPT (Zenkour 2007)	=0	0.28399	0.30379	0.32483	0.34719	0.38338	0.45159

Table 5 Continued

b/a	Theory	ε_z	p					
			0.1	0.3	0.5	0.7	1.0	1.5
3	3-D (Zenkour 2007)	≠0	0.23188	0.24692	0.26295	0.28002	0.30775	0.36021
	Present	≠0	0.22671	0.24082	0.25604	0.27247	0.29973	0.35322
	Present	=0	0.21618	0.23121	0.24718	0.26416	0.29164	0.34345
	Mantari and Soares (2013)	≠0	0.22721	0.24137	0.25663	0.27312	0.30044	0.35404
	Mantari and Soares (2012)	=0	0.21619	0.23122	0.24720	0.26417	0.29166	0.34346
	TPT (Zenkour 2007)	≠0	0.24931	0.26563	0.28307	0.30174	0.33230	0.39106
	HPT (Zenkour 2007)	=0	0.28588	0.30583	0.32702	0.34954	0.38601	0.45471
2	3-D (Zenkour 2007)	≠0	0.24314	0.25913	0.27618	0.29434	0.32385	0.37968
	Present	≠0	0.23910	0.25449	0.27102	0.28879	0.31807	0.37489
	Present	=0	0.22942	0.24540	0.26238	0.28043	0.30965	0.36471
	Mantari and Soares (2013)	≠0	0.23953	0.25497	0.27154	0.28936	0.3187	0.37562
	Mantari and Soares (2012)	=0	0.22943	0.24542	0.26240	0.28045	0.30967	0.36473
	TPT (Zenkour 2007)	≠0	0.25878	0.27609	0.29456	0.31428	0.34644	0.40788
	HPT (Zenkour 2007)	=0	0.28539	0.30534	0.32655	0.34908	0.38556	0.45428
1	3-D (Zenkour 2007)	≠0	0.22472	0.23995	0.25621	0.27356	0.30177	0.35885
	Present	≠0	0.22346	0.23879	0.25514	0.27258	0.30101	0.35513
	Present	=0	0.21634	0.23155	0.24772	0.26490	0.29270	0.34505
	Mantari and Soares (2013)	≠0	0.22372	0.23907	0.25544	0.27291	0.30137	0.35555
	Mantari and Soares (2012)	=0	0.21636	0.23157	0.24774	0.26492	0.29273	0.34508
	TPT (Zenkour 2007)	≠0	0.23457	0.25098	0.26842	0.28698	0.31706	0.37386
	HPT (Zenkour 2007)	=0	0.24080	0.25783	0.27593	0.29515	0.32627	0.38482

Table 6 Non-dimensional axial stress $\bar{\sigma}_{yy}$ (*a*/2, *b/2*, *h/2*) for various EG plates, *a/h*=10

b/a	Theory	ε_z	p								
			0.1	0.3	0.5	0.7	1.0	1.5	2.0	2.5	3.0
6	Present	≠0	0.1948	0.2058	0.2178	0.2310	0.2531	0.2978	0.3541	0.4243	0.5102
	Present	=0	0.1960	0.2094	0.2237	0.2389	0.2635	0.3100	0.3642	0.4275	0.5011
	Mantari and Soares (2013)	≠0	0.1954	0.2065	0.2185	0.2317	0.2540	0.2988	0.3552	0.4255	0.5115
	Mantari and Soares (2012)	=0	0.1960	0.2094	0.2237	0.2389	0.2635	0.3100	0.3642	0.4275	0.5011
	TPT (Mantari and Soares 2013)	≠0	0.2223	0.2360	0.2507	0.2665	0.2926	0.3435	0.4054	0.4805	0.5708
5	Present	≠0	0.1974	0.2086	0.2209	0.2343	0.2568	0.3021	0.3591	0.4300	0.5166
	Present	=0	0.1985	0.2122	0.2267	0.2421	0.2670	0.3140	0.3690	0.4331	0.5077
	Mantari and Soares (2013)	≠0	0.1980	0.2093	0.2216	0.2350	0.2577	0.3031	0.3602	0.4312	0.5179
	Mantari and Soares (2012)	=0	0.1985	0.2122	0.2267	0.2421	0.2670	0.3140	0.3690	0.4331	0.5077
	TPT (Mantari and Soares 2013)	≠0	0.2245	0.2385	0.2534	0.2694	0.2958	0.3473	0.4098	0.4855	0.5764

Table 6 Continued

b/a	Theory	ε_z	p								
			0.1	0.3	0.5	0.7	1.0	1.5	2.0	2.5	3.0
4	Present	≠0	0.2017	0.2134	0.2260	0.2398	0.2630	0.3094	0.3676	0.4395	0.5273
	Present	=0	0.2028	0.2168	0.2316	0.2473	0.2728	0.3208	0.3770	0.4424	0.5187
	Mantari and Soares (2013)	≠0	0.2023	0.2140	0.2267	0.2406	0.2638	0.3104	0.3686	0.4407	0.5285
	Mantari and Soares (2012)	=0	0.2028	0.2168	0.2316	0.2473	0.2728	0.3208	0.3770	0.4424	0.5187
	TPT(Mantari and Soares 2013)	≠0	0.2283	0.2425	0.2578	0.2742	0.3012	0.3535	0.4170	0.4937	0.5857
3	Present	≠0	0.2094	0.2218	0.2352	0.2497	0.2740	0.3224	0.3825	0.4563	0.5460
	Present	=0	0.2104	0.2248	0.2402	0.2565	0.2829	0.3328	0.3910	0.4590	0.5380
	Mantari and Soares (2013)	≠0	0.2099	0.2224	0.2358	0.2504	0.2748	0.3233	0.3835	0.4575	0.5472
	Mantari and Soares (2012)	=0	0.2104	0.2248	0.2402	0.2565	0.2829	0.3328	0.3910	0.4589	0.5380
	TPT (Mantari and Soares 2013)	≠0	0.2347	0.2495	0.2654	0.2825	0.3104	0.3645	0.4296	0.5080	0.6016
2	Present	≠0	0.2218	0.2354	0.2501	0.2660	0.2923	0.3439	0.4070	0.4836	0.5757
	Present	=0	0.2225	0.2378	0.2541	0.2713	0.2993	0.3521	0.4137	0.4855	0.5692
	Mantari and Soares (2013)	≠0	0.2223	0.2360	0.2507	0.2666	0.2930	0.3447	0.4079	0.4846	0.5768
	Mantari and Soares (2012)	=0	0.2225	0.2378	0.2541	0.2713	0.2993	0.3521	0.4137	0.4855	0.5692
	TPT (Mantari and Soares 2013)	≠0	0.2441	0.2599	0.2768	0.2949	0.3244	0.3810	0.4486	0.5291	0.6246
1	Present	≠0	0.2060	0.2195	0.2340	0.2495	0.2749	0.3235	0.3813	0.4499	0.5309
	Present	=0	0.2062	0.2204	0.2355	0.2515	0.2774	0.3264	0.3835	0.4502	0.5277
	Mantari and Soares (2013)	≠0	0.2063	0.2199	0.2344	0.2499	0.2753	0.3240	0.3819	0.4506	0.5317
	Mantari and Soares (2012)	=0	0.2062	0.2204	0.2355	0.2515	0.2774	0.3264	0.3835	0.4502	0.5278
	TPT (Mantari and Soares 2013)	≠0	0.2196	0.2345	0.2503	0.2671	0.2944	0.3460	0.4065	0.4775	0.5603

ratio (*a/h*=2, 4, 10) and for various values of both aspect ratio a/b and material parameter p.

Tables 7-8 also show the comparison of axial normal stress $\bar{\sigma}_x$ and transverse shear stress $\bar{\tau}_{xz}$, respectively for simply supported, moderately thick rectangular EG plates (*a/h* = 10). It is evident from the results that the present computations are in an excellent agreement with the 2D and quasi-3D solutions provided by Mantari and Guedes Soares (2012, 2013). However, it can be noticed that the decrease of the parameter values *p* and the increase of the thickness ratio *a/h* have a significant effect on the reduction of the axial normal stress $\bar{\sigma}_y$ for all the cases presented.

On the other hand, according to the analytical solutions given in Tables 7-8, it can be seen again that the axial normal stress $\bar{\sigma}_x$ increase with both the increase of the parameter *p* and the increase of aspect ratio *b/a*. Whereas, the transverse shear stress $\bar{\tau}_{xz}$ decrease with the increase of the

Table 7 Non-dimensional axial stress $\bar{\sigma}_{xx}$ ($a/2$, $b/2$, $h/2$) for various EG plates, a/h=10

b/a	Theory	ε_z	p								
			0.1	0.3	0.5	0.7	1.0	1.5	2.0	2.5	3.0
6	Present	$\neq 0$	0.6008	0.6419	0.6856	0.7321	0.8075	0.9500	1.1166	1.3113	1.5382
	Present	$= 0$	0.6029	0.6443	0.6882	0.7350	0.8107	0.9536	1.1204	1.3150	1.5416
	Mantari and Soares (2013)	$\neq 0$	0.6014	0.6426	0.6864	0.7329	0.8084	0.9510	1.1177	1.3124	1.5394
	Mantari and Soares (2012)	$= 0$	0.6029	0.6443	0.6882	0.7350	0.8107	0.9536	1.1204	1.3150	1.5415
	TPT (Mantari and Soares 2013)	$\neq 0$	0.6271	0.6707	0.7170	0.7661	0.8452	0.9935	1.1651	1.3637	1.5935
5	Present	$\neq 0$	0.5889	0.6292	0.6720	0.7176	0.7915	0.9311	1.0944	1.2854	1.5080
	Present	$= 0$	0.5910	0.6315	0.6746	0.7205	0.7947	0.9347	1.0982	1.2890	1.5112
	Mantari and Soares (2013)	$\neq 0$	0.5895	0.6299	0.6727	0.7184	0.7923	0.9321	1.0955	1.2865	1.5091
	Mantari and Soares (2012)	$= 0$	0.5910	0.6315	0.6746	0.7205	0.7947	0.9347	1.0982	1.2890	1.5111
	TPT (Mantari and Soares 2013)	$\neq 0$	0.6149	0.6577	0.7031	0.7512	0.8287	0.9741	1.1424	1.3372	1.5626
4	Present	$\neq 0$	0.5680	0.6069	0.6481	0.6920	0.7632	0.8979	1.0555	1.2398	1.4548
	Present	$= 0$	0.5700	0.6092	0.6508	0.6950	0.7666	0.9016	1.0594	1.2434	1.4577
	Mantari and Soares (2013)	$\neq 0$	0.5686	0.6075	0.6488	0.6928	0.7641	0.8989	1.0566	1.2410	1.4560
	Mantari and Soares (2012)	$= 0$	0.5700	0.6092	0.6508	0.6950	0.7666	0.9016	1.0594	1.2434	1.4576
	TPT (Mantari and Soares 2013)	$\neq 0$	0.5935	0.6348	0.6785	0.7249	0.7998	0.9401	1.1025	1.2907	1.5084
3	Present	$\neq 0$	0.5270	0.5629	0.6011	0.6418	0.7077	0.8326	0.9790	1.1503	1.3502
	Present	$= 0$	0.5288	0.5651	0.6037	0.6447	0.7112	0.8365	0.9828	1.1536	1.3524
	Mantari and Soares (2013)	$\neq 0$	0.5275	0.5635	0.6018	0.6425	0.7085	0.8335	0.9800	1.1514	1.3514
	Mantari and Soares (2012)	$= 0$	0.5288	0.5651	0.6037	0.6447	0.7112	0.8365	0.9828	1.1536	1.3523
	TPT (Mantari and Soares 2013)	$\neq 0$	0.5514	0.5896	0.6302	0.6733	0.7427	0.8730	1.0240	1.1990	1.4017

parameter p and the decrease of aspect ratio b/a (see Table 8). It may be noted here that the aim of this research is to verify the accuracy of the present high-order model in predicting the bending response of rectangular FG plates for two different cases, in which the stretching effect is considered or neglected.

5. Conclusions

The present work focused on a new kinematics which is modeled with an undetermined integral

Table 7 Continued

b/a	Theory	ε_z	*p*								
			0.1	0.3	0.5	0.7	1.0	1.5	2.0	2.5	3.0
2	Present	$\neq 0$	0.4335	0.4628	0.4941	0.5274	0.5815	0.6841	0.8047	0.9463	1.1119
	Present	$= 0$	0.4350	0.4649	0.4966	0.5303	0.5850	0.6881	0.8085	0.9490	1.1125
	Mantari and Soares (2013)	$\neq 0$	0.4340	0.4634	0.4947	0.5280	0.5822	0.6849	0.8056	0.9473	1.1130
	Mantari and Soares (2012)	$= 0$	0.4350	0.4649	0.4966	0.5303	0.5850	0.6881	0.8085	0.9490	1.1125
	TPT (Mantari and Soares 2013)	$\neq 0$	0.4552	0.4867	0.5200	0.5554	0.6126	0.7201	0.8449	0.9898	1.1580
1	Present	$\neq 0$	0.2060	0.2195	0.2340	0.2495	0.2749	0.3234	0.3813	0.4499	0.5309
	Present	$= 0$	0.2062	0.2204	0.2355	0.2515	0.2774	0.3264	0.3835	0.4502	0.5277
	Mantari and Soares (2013)	$\neq 0$	0.2063	0.2199	0.2344	0.2499	0.2753	0.3240	0.3819	0.4506	0.5317
	Mantari and Soares (2012)	$= 0$	0.2062	0.2204	0.2355	0.2515	0.2774	0.3264	0.3835	0.4502	0.5278
	TPT (Mantari and Soares 2013)	$\neq 0$	0.2196	0.2345	0.2503	0.2671	0.2944	0.3460	0.4065	0.4775	0.5603

Table 8 Non-dimensional transverse shear stress $\bar{\tau}_{xz}$ (0, *b/2*, 0) for various EG plates, *a/h*=10

b/a	Theory	ε_z	*p*								
			0.1	0.3	0.5	0.7	1.0	1.5	2.0	2.5	3.0
6	Present	$\neq0$	0.4630	0.4622	0.4607	0.4583	0.4533	0.4413	0.4250	0.4051	0.3821
	Present	$=0$	0.4629	0.4621	0.4605	0.4582	0.4532	0.4412	0.4249	0.4050	0.3820
	Mantari and Soares (2013)	$\neq0$	0.4634	0.4626	0.4610	0.4586	0.4536	0.4416	0.4253	0.4065	0.3845
	Mantari and Soares (2012)	$=0$	0.4633	0.4625	0.4609	0.4585	0.4536	0.4415	0.4252	0.4064	0.3842
	TPT (Mantari and Soares 2013)	$\neq0$	0.4776	0.4769	0.4753	0.4730	0.4681	0.4564	0.4405	0.4209	0.3981
5	Present	$\neq0$	0.4576	0.4568	0.4552	0.4529	0.4479	0.4361	0.4200	0.4003	0.3776
	Present	$=0$	0.4575	0.4567	0.4551	0.4528	0.4478	0.4360	0.4199	0.4002	0.3775
	Mantari and Soares (2013)	$\neq0$	0.4579	0.4571	0.4556	0.4532	0.4483	0.4364	0.4203	0.4017	0.3800
	Mantari and Soares (2012)	$=0$	0.4579	0.4571	0.4555	0.4531	0.4482	0.4363	0.4202	0.4016	0.3797
	TPT (Mantari and Soares 2013)	$\neq0$	0.4720	0.4713	0.4697	0.4674	0.4626	0.4510	0.4353	0.4159	0.3935
4	Present	$\neq0$	0.4479	0.4471	0.4456	0.4433	0.4385	0.4268	0.4111	0.3918	0.3696
	Present	$=0$	0.4478	0.4470	0.4455	0.4432	0.4384	0.4267	0.4110	0.3917	0.3695
	Mantari and Soares (2013)	$\neq0$	0.4482	0.4475	0.4459	0.4436	0.4388	0.4271	0.4114	0.3933	0.3720
	Mantari and Soares (2012)	$=0$	0.4482	0.4474	0.4458	0.4435	0.4387	0.4271	0.4113	0.3931	0.3717
	TPT (Mantari and Soares 2013)	$\neq0$	0.4620	0.4613	0.4598	0.4575	0.4528	0.4415	0.4261	0.4071	0.3851

Table 8 Continued

b/a	Theory	ε_z	*p*								
			0.1	0.3	0.5	0.7	1.0	1.5	2.0	2.5	3.0
3	Present	≠0	0.4283	0.4276	0.4261	0.4239	0.4193	0.4082	0.3931	0.3747	0.3534
	Present	=0	0.4282	0.4275	0.4260	0.4238	0.4192	0.4081	0.3930	0.3746	0.3533
	Mantari and Soares (2013)	≠0	0.4286	0.4279	0.4264	0.4242	0.4196	0.4084	0.3934	0.3761	0.3558
	Mantari and Soares (2012)	=0	0.4285	0.4278	0.4263	0.4241	0.4195	0.4084	0.3933	0.3760	0.3555
	TPT (Mantari and Soares 2013)	≠0	0.4418	0.4411	0.4396	0.4375	0.4330	0.4221	0.4074	0.3893	0.3683
2	Present	≠0	0.3807	0.3800	0.3787	0.3768	0.3727	0.3628	0.3494	0.3330	0.3141
	Present	=0	0.3806	0.3800	0.3786	0.3767	0.3726	0.3627	0.3493	0.3330	0.3141
	Mantari and Soares (2013)	≠0	0.3810	0.3803	0.3790	0.3770	0.3730	0.3630	0.3497	0.3344	0.3165
	Mantari and Soares (2012)	=0	0.3809	0.3803	0.3789	0.3770	0.3729	0.3630	0.3496	0.3343	0.3162
	TPT (Mantari and Soares 2013)	≠0	0.3927	0.3921	0.3908	0.3889	0.3849	0.3752	0.3621	0.3460	0.3273
1	Present	≠0	0.2379	0.2375	0.2366	0.2354	0.2328	0.2267	0.2183	0.2081	0.1962
	Present	=0	0.2378	0.2374	0.2366	0.2354	0.2328	0.2266	0.2183	0.2080	0.1962
	Mantari and Soares (2013)	≠0	0.2380	0.2376	0.2368	0.2356	0.2330	0.2268	0.2185	0.2094	0.1985
	Mantari and Soares (2012)	=0	0.2380	0.2376	0.2368	0.2356	0.2330	0.2268	0.2184	0.2093	0.1983
	TPT (Mantari and Soares 2013)	≠0	0.2454	0.2450	0.2442	0.2430	0.2405	0.2344	0.2263	0.2162	0.2045

component for the bending analysis of rectangular exponentially graded plates based on both hyperbolic quasi-3D and 2D higher-order shear deformation theories. The theories are variationally consistent and does not require shear correction factor. It should be recalled that the first theory (quasi-3D HySDT) contains only five unknowns and five governing equations in which both shear deformation and thickness stretching effects are included, while the second theory (2D HySDT) without including the stretching effect and contains only four unknowns and four governing equations. However, the static problem under consideration are solved analytically by using Navier'is solution method to obtained closed form solution for displacements and stresses of simply supported rectangular EG plates subjected to sinusoidal distributed load for various material parameter, side-to-thickness ratio and aspect ratio. The numerical results obtained by using the present formulation are verified with the published results available in the open literature. As expected, it can be stated that the proposed theories predicts more accurate transverse shear stresses than those provided by other refined theories as compared to exact values. An improvement of the present formulation will be considered in the future work to consider other type of materials (Daouadji 2017, Shahsavari and Janghorban 2017,

Panjehpour *et al.* 2018, Ayat *et al.* 2018, Akbaş 2018b and 2019, Draoui *et al*. 2019, Karami *et al*. 2019d, Hussain *et al*. 2019, Medani *et al*. 2019, Semmah *et al*. 2019).

Acknowledgments

Author would like to acknowledge the support provided by the Directorate General for Scientific Research and Technological Development (DGRSDT).

References

Abualnour, M., Chikh, A., Hebali, H., Kaci, A., Tounsi, A., Bousahla, A.A. and Tounsi, A. (2019), "Thermomechanical analysis of antisymmetric laminated reinforced composite plates using a new four variable trigonometric refined plate theory", *Comput. Concrete*, **24**(6), 489-498. https://doi.org/10.12989/cac.2019.24.6.489.

Adda Bedia, W., Houari, M.S.A., Bessaim, A., Bousahla, A.A., Tounsi, A., Saeed, T. and Alhodaly, M.Sh. (2019), "A new hyperbolic two-unknown beam model for bending and buckling analysis of a nonlocal strain gradient nanobeams", *J. Nano Res.*, **57**, 175-191. https://doi.org/10.4028/www.scientific.net/JNanoR.57.175.

Ahmed, A. (2014), "Post buckling analysis of sandwich beams with functionally graded faces using a consistent higher order theory", *Int. J. Civil Struct. Environ.*, **4**(2), 59-64.

Akavci, S.S. and Tanrikulu, A.H. (2015), "Static and free vibration analysis of functionally graded plates based on a new quasi-3D and 2D shear deformation theories", *Compos. Part B*, **83**, 203-215. https://doi.org/10.1016/j.compositesb.2015.08.043.

Akbaş, Ş.D. (2018a), "Forced vibration analysis of functionally graded porous deep beams", *Compos. Struct.*, **186**, 293-302. https://doi.org/10.1016/j.compstruct.2017.12.013.

Akbaş, Ş.D. (2018b), "Nonlinear thermal displacements of laminated composite beams", *Coupl. Syst. Mech.*, **7**(6), 691-705. https://doi.org/10.12989/csm.2018.7.6.691.

Akbaş, Ş.D. (2019), "Forced vibration analysis of functionally graded sandwich deep beams", *Coupl. Syst. Mech.*, **8**(3), 259-271. http://dx.doi.org/10.12989/csm.2019.8.3.259.

Aldousari, S.M. (2017), "Bending analysis of different material distributions of functionally graded beam", *Appl. Phys. A*, **123**, 296. https://doi.org/10.1007/s00339-017-0854-0.

Alimirzaei, S., Mohammadimehr, M. and Tounsi, A. (2019), "Nonlinear analysis of viscoelastic micro-composite beam with geometrical imperfection using FEM: MSGT electro-magneto-elastic bending, buckling and vibration solutions", *Struct. Eng. Mech.*, **71**(5), 485-502. https://doi.org/10.12989/sem.2019.71.5.485.

Avcar, M. (2019), "Free vibration of imperfect sigmoid and power law functionally graded beams", *Steel Compos. Struct.*, **30**(6), 603-615. https://doi.org/10.12989/scs.2019.30.6.603.

Avcar, M. and Alwan, A.S. (2017), "Free vibration of functionally graded Rayleigh beam", *Int. J. Eng. Appl. Sci.*, **9**(2), 127-127. https://doi.org/10.24107/ijeas.322884.

Avcar, M. and Mohammed, W.K.M. (2018), "Free vibration of functionally graded beams resting on Winkler-Pasternak foundation", *Arab. J. Geosci.*, **11**(10), 232. https://doi.org/10.1007/s12517-018-3579-2.

Ayat, H., Kellouche, Y., Ghrici, M. and Boukhatem, B. (2018), "Compressive strength prediction of limestone filler concrete using artificial neural networks", *Adv. Comput. Des.*, **3**(3), 289-302. https://doi.org/10.12989/acd.2018.3.3.289.

Balubaid, M., Tounsi, A., Dakhel, B. and Mahmoud, S.R. (2019), "Free vibration investigation of FG nanoscale plate using nonlocal two variables integral refined plate theory", *Comput. Concrete*, **24**(6), 579-586. https://doi.org/10.12989/cac.2019.24.6.579.

Batou, B., Nebab, M., Bennai, R., Ait Atmane, H., Tounsi, A. and Bouremana, M. (2019), "Wave dispersion properties in imperfect sigmoid plates using various HSDTs", *Steel Compos. Struct.*, **33**(5), 699-716. https://doi.org/10.12989/scs.2019.33.5.699.

Birman, V. and Byrd, L.W. (2007), "Modeling and analysis of functionally graded materials and structures", *Appl. Mech. Rev. ASME*, **60**, 195-216. https://doi.org/10.1115/1.2777164.

Bisen, H.B., Hirwani, C.K., Satankar, R.K., Panda, S.K., Mehar, K. and Patel, B. (2018), "Numerical study of frequency and deflection responses of natural fiber (Luffa) reinforced polymer composite and experimental validation", *J. Nat. Fib*., **17**(4), 505-519. https://doi.org/10.1080/15440478.2018.1503129.

Boulefrakh, L., Hebali, H., Chikh, A., Bousahla, A.A., Tounsi, A. and Mahmoud, S.R. (2019), "The effect of parameters of visco-Pasternak foundation on the bending and vibration properties of a thick FG plate", *Geomech. Eng.*, **18**(2), 161-178. https://doi.org/10.12989/gae.2019.18.2.161.

Boutaleb, S., Benrahou, K.H., Bakora, A., Algarni, A., Bousahla, A.A., Tounsi, A., Mahmoud, S.R. and Tounsi, A. (2019), "Dynamic Analysis of nanosize FG rectangular plates based on simple nonlocal quasi 3D HSDT", *Adv. Nano Res.*, **7**(3), 189-206. https://doi.org/10.12989/anr.2019.7.3.191.

Carrera, E., Brischetto, S. and Robaldo, A. (2008), "A variable kinematic model for the analysis of functionally graded materials plates", *AIAA J.*, **46**, 194-203. https://doi.org/10.2514/1.32490.

Carrera, E., Brischetto, S., Cinefra, M. and Soave, M. (2011), "Effects of thickness stretching in functionally graded plates and shells", *Compos. Part B*, **42**, 123-33. https://doi.org/10.1016/j.compositesb.2010.10.005.

Cheng, Z.Q. and Batra, R.C. (2000), "Exact correspondence between eigenvalues of membranes and functionally graded simply supported polygonal plates", *J. Sound Vib.*, **229**, 879-895. https://doi.org/10.1006/jsvi.1999.2525.

Chi, S.H. and Chung, Y.L. (2006), "Mechanical behavior of functionally graded material plates under transverse load-Part I: Analysis", *Int. J. Solid. Struct.*, **43**, 3657-3674. https://doi.org/10.1016/j.ijsolstr.2005.04.011.

Daouadji, T.H. (2017), "Analytical and numerical modeling of interfacial stresses in beams bonded with a thin plate", *Adv. Comput. Des.*, **2**(1), 57-69. https://doi.org/10.12989/acd.2017.2.1.057.

Daouadji, T.H. and Hadji, L. (2015), "Analytical solution of nonlinear cylindrical bending for functionally graded plates", *Geomech. Eng.*, **9**(5), 631-644. https://doi.org/10.12989/gae.2015.9.5.631.

Daouadji, T.H., Benferhat, R. and Adim, B. (2016), "Bending analysis of an imperfect advanced composite plates resting on the elastic foundations", *Coupl. Syst. Mech.*, **5**(3), 269-283. https://doi.org/10.12989/csm.2016.5.3.269.

Draiche, K., Bousahla, A.A., Tounsi, A., Alwabli, A.S., Tounsi, A. and Mahmoud, S.R. (2019), "Static analysis of laminated reinforced composite plates using a simple first-order shear deformation theory", *Comput. Concrete*, **24**(4), 369-378. https://doi.org/10.12989/cac.2019.24.4.369.

Draoui, A., Zidour, M., Tounsi, A. and Adim, B. (2019), "Static and dynamic behavior of nanotubes-reinforced sandwich plates using (FSDT)", *J. Nano Res.*, **57**, 117-135. https://doi.org/10.4028/www.scientific.net/JNanoR.57.117.

Eltaher, M.A., Fouda, N., El-Midany, T. and Sadoun, A.M. (2018), "Modified porosity model in analysis of functionally graded porous nanobeams", *J. Brazil. Soc. Mech. Sci. Eng.*, **40**, 141. https://doi.org/10.1007/s40430-018-1065-0.

Faleh, N.M., Ahmed, R.A. and Fenjan, R.M. (2018), "On vibrations of porous FG nanoshells", *Int. J. Eng. Sci.*, **133**, 1-14. https://doi.org/10.1016/j.ijengsci.2018.08.007.

Ferreira, A.J.M, Batra, R.C. and Roque, C.M.C. (2005), "Static analysis of functionally graded plates using third-order shear deformation theory and a meshless method", *Compos. Struct.*, **69**, 449-457. https://doi.org/10.1016/j.compstruct.2004.08.003.

Gandra, J., Miranda, R., Vilaça, P., Velhinho, A. and Pamies Teixeira, J. (2011), "Functionally graded materials produced by friction stir processing", *J. Mater. Process. Tech.*, **211**, 1659-1668. https://doi.org/10.1016/j.jmatprotec.2011.04.016.

Hussain, M. and Naeem, M.N. (2019), "Rotating response on the vibrations of functionally graded zigzag and chiral single walled carbon nanotubes", *Appl. Math. Model.*, **75**, 506-520. https://doi.org/10.1016/j.apm.2019.05.039.

Hussain, M., Naeem, M.N., Tounsi, A. and Taj, M. (2019), "Nonlocal effect on the vibration of armchair and zigzag SWCNTs with bending rigidity", *J. Nano Res.*, **7**(6), 431-442. https://doi.org/10.12989/anr.2019.7.6.431.

Javaheri, R. and Eslami, M.R. (2002), "Thermal buckling of functionally graded plates", *AIAA J.*, **40** (1), 162-169. https://doi.org/10.2514/2.1626.

Jha, D.K., Kant, T. and Singh, R.K. (2013), "A critical review of recent research on functionally graded plates", *Compos. Struct.*, **96**, 833-849. https://doi.org/10.1016/j.compstruct.2012.09.001.

Kar, V.R. and Panda, S.K. (2015), "Nonlinear flexural vibration of shear deformable functionally graded spherical shell panel", *Steel Compos. Struct.*, **18**(3), 693-709. https://doi.org/10.12989/scs.2015.18.3.693.

Karami, B., Janghorban, M. and Tounsi, A. (2019a), "Galerkin'is approach for buckling analysis of functionally graded anisotropic nanoplates/different boundary conditions", *Eng. Comput.*, **35**, 1297-1316. https://doi.org/10.1007/s00366-018-0664-9.

Karami, B., Janghorban, M. and Tounsi, A. (2019b), "Wave propagation of functionally graded anisotropic nanoplates resting on Winkler-Pasternak foundation", *Struct. Eng. Mech.*, **7**(1), 55-66. https://doi.org/10.12989/sem.2019.70.1.055.

Karami, B., Janghorban, M. and Tounsi, A. (2019d), "On exact wave propagation analysis of triclinic material using three dimensional bi-Helmholtz gradient plate model", *Struct. Eng. Mech.*, **69**(5), 487-497. https://doi.org/10.12989/sem.2019.69.5.487.

Karami, B., Janghorban, M. and Tounsi, A. (2019e), "On pre-stressed functionally graded anisotropic nanoshell in magnetic field", *J. Brazil. Soc. Mech. Sci. Eng.*, **41**, 495. https://doi.org/10.1007/s40430-019-1996-0.

Karami, B., Shahsavari, D. and Janghorban, M. (2018), "Wave propagation analysis in functionally graded (FG) nanoplates under in-plane magnetic field based on nonlocal strain gradient theory and four variable refined plate theory", *Mech. Adv. Mater. Struct.*, **25**(12), 1047-1057. https://doi.org/10.1080/15376494.2017.1323143.

Karami, B., Shahsavari, D., Janghorban, M. and Tounsi, A. (2019c), "Resonance behavior of functionally graded polymer composite nanoplates reinforced with grapheme nanoplatelets", *Int. J. Mech. Sci.*, **156**, 94-105. https://doi.org/10.1016/j.ijmecsci.2019.03.036.

Kawasaki, A. and Watanabe, R. (1997), "Concept and P/M fabrication of functionally gradient materials", *Ceram. Int. J.*, **23**, 73-83. https://doi.org/10.1016/0272-8842(95)00143-3.

Khiloun, M., Bousahla, A.A., Kaci, A., Bessaim, A., Tounsi, A. and Mahmoud, S.R. (2019), "Analytical modeling of bending and vibration of thick advanced composite plates using a four-variable quasi 3D HSDT", *Eng. Comput*., https://doi.org/10.1007/s00366-019-00732-1.

Koizumi, M. (1993), "The concept of FGM", *Ceram. Trans.*, **34**, 3-10.

Koizumi, M. (1997), "FGM activities in Japan", *Compos. Part B Eng.*, **28**, 1-4. https://doi.org/10.1016/S1359-8368(96)00016-9.

Kolahchi, R., Bidgoli, A.M.M. and Heydari, M.M. (2015), "Size-dependent bending analysis of FGM nano-sinusoidal plates resting on orthotropic elastic medium", *Struct. Eng. Mech.*, **55**(5), 1001-1014. http://dx.doi.org/10.12989/sem.2015.55.5.1001.

Kumar, S. (2010), "Development of functionally graded materials by ultrasonic consolidation", *CIRP J. Manuf. Sci. Tech.*, **3**, 85-87. https://doi.org/10.1016/j.cirpj.2010.07.006.

Lal, A., Jagtap, K.R. and Singh, B.N. (2017), "Thermo-mechanically induced finite element based nonlinear static response of elastically supported functionally graded plate with random system properties", *Adv. Comput. Des.*, **2**(3), 165-194. https://doi.org/10.12989/acd.2017.2.3.165.

Laoufi, I., Ameur, M., Zidi, M., Adda Bedia, E.A. and Bousahla, A.A. (2016), "Mechanical and hygrothermal behaviour of functionally graded plates using a hyperbolic shear deformation theory", *Steel Compos. Struct.*, **20**(4), 889-911. https://doi.org/10.12989/scs.2016.20.4.889.

Mahamood, R.M. and Akinlabi, E.T. (2017), *Functionally Graded Materials*, Springer International Publishing AG, 118.

Mahmoudi, A., Benyoucef, S., Tounsi, A., Benachour, A., Adda Bedia, E.A. and Mahmoud, S.R. (2019), "A refined quasi-3D shear deformation theory for thermo-mechanical behavior of functionally graded sandwich plates on elastic foundations", *J. Sandw. Struct. Mater.*, **21**(6), 1906-1926. https://doi.org/10.1177/1099636217727577.

Mantari, J.L. and Guedes Soares, C. (2012), "Generalized hybrid quasi-3D shear deformation theory for the static analysis of advanced composite plates", *Compos. Struct.*, **94**, 2561-2575. https://doi.org/10.1016/j.compstruct.2012.02.019.

Mantari, J.L. and Guedes Soares, C. (2013), "A novel higher-order shear deformation theory with stretching effect for functionally graded plates", *Compos.: Part B*, **45**, 268-281. https://doi.org/10.1016/j.compositesb.2012.05.036.

Mantari, J.L. and Guedes Soares, C. (2014), "A trigonometric plate theory with 5-unknowns and stretching effect for advanced composite plates", *Compos. Struct.*, **107**, 396-405. https://doi.org/10.1016/j.compstruct.2013.07.046.

Medani, M., Benahmed, A., Zidour, M., Heireche, H., Tounsi, A., Bousahla, A.A., Tounsi, A. and Mahmoud, S.R. (2019), "Static and dynamic behavior of (FG-CNT) reinforced porous sandwich plate", *Steel Compos. Struct.*, **32**(5), 595-610. https://doi.org/10.12989/scs.2019.32.5.595.

Mehar, K. and Panda, S.K. (2016), "Free vibration and bending behaviour of CNT reinforced composite plate using different shear deformation theory", *IOP Conf. Ser.: Mater. Sci. Eng.*, **115**(1), 012014. https://doi.org/10.1088/1757-899X/115/1/012014.

Mehar, K. and Panda, S.K. (2018), "Elastic bending and stress analysis of carbon nanotube-reinforced composite plate: Experimental, numerical, and simulation", *Adv. Polym. Technol.*, **37**(6), 1643-1657. https://doi.org/10.1002/adv.21821.

Mehar, K. and Panda, S.K. (2019), "Theoretical deflection analysis of multi-walled carbon nanotube reinforced sandwich panel and experimental verification", *Compos. Part B: Eng.*, **167**, 317-328. https://doi.org/10.1016/j.compositesb.2018.12.058.

Mehar, K., Panda, S.K. and Mahapatra, T.R. (2019), "Large deformation bending responses of nanotube-reinforced polymer composite panel structure: Numerical and experimental analyses", *Proc. Inst. Mech. Eng., Part G: J. Aerosp. Eng.*, **233**(5), 1695-1704. https://doi.org/10.1177/0954410018761192.

Meksi, R, Benyoucef, S., Mahmoudi, A., Tounsi, A., Adda Bedia, E.A. and Mahmoud, SR. (2019), "An analytical solution for bending, buckling and vibration responses of FGM sandwich plates", *J. Sandw. Struct. Mater.*, **21**(2), 727-757. https://doi.org/10.1177/1099636217698443.

Miyamoto, Y. (2016), "The applications of functionally graded materials in Japan", *Mater. Tech.*, **11**(6), 230-236. https://doi.org/10.1080/10667857.1996.11752708.

Muller, E., Drasar, C., Schilz, J. and Kaysser, W.A. (2003), "Functionally graded materials for sensor and energy applications", *J. Mater. Sci. Eng.: A*, **362**, 17-39. https://doi.org/10.1016/S0921-5093(03)00581-1.

Neves, A.M.A., Ferreira, A.J.M., Carrera, E., Cinefra, M., Roque, C.M.C., Jorge, R.M.N. and Soares, C.M. (2013), "Static, free vibration and buckling analysis of isotropic and sandwich functionally graded plates using a quasi-3D higher-order shear deformation theory and a meshless technique", *Compos. Part B Eng.*, **44**(1), 657-674. https://doi.org/10.1016/j.compositesb.2012.01.089.

Nguyen, K.T., Thai, H.T. and Vo, T.P. (2015), "A refined higher-order shear deformation theory for bending, vibration and buckling analysis of functionally graded sandwich plates", *Steel Compos. Struct.*, **18**(1), 91-120. http://dx.doi.org/10.12989/scs.2015.18.1.091.

Pindera, M.J., Aboudi, J., Glaeser, A.M. and Arnolds, S.M. (1997), "Use of composites in multi-phased and functionally graded materials", *Compos. Part B*, **28**, 1-175.

Pompe, W., Worch, H., Epple, M., Friess, W., Gelinsky, M., Greil, P., Hempel, U., Scharnweber, D. and Schulte, K. (2003), "Functionally graded materials for biomedical applications", *Mater. Sci. Eng.: A*, **362**(1), 40-60. https://doi.org/10.1016/S0921-5093(03)00580-X.

Qian, L.F., Batra, R.C. and Chen, L.M. (2004), "Static and dynamic deformations of thick functionally graded elastic plates by using higher-order shear and normal deformable plate theory and meshless local Petrov-Galerkin method", *Compos. Part B*, **35**, 685-697. https://doi.org/10.1016/j.compositesb.2004.02.004.

Reddy, J.N. (2000), "Analysis of functionally graded plates", *Int. J. Numer. Meth. Eng.*, **47**, 663-684. https://doi.org/10.1002/(SICI)1097-0207(20000110/30)47:1/3<663::AID-NME787>3.0.CO;2-8.

Rezaiee-Pajand, M., Masoodi, A.R. and Mokhtari, M. (2018), "Static analysis of functionally graded non-prismatic sandwich beams", *Adv. Comput. Des.*, **3**(2), 165-190. https://doi.org/10.12989/acd.2018.3.2.165.

Salah, F., Boucham, B., Bourada, F., Benzair, A., Bousahla, A.A. and Tounsi, A. (2019), "Investigation of thermal buckling properties of ceramic-metal FGM sandwich plates using 2D integral plate model", *Steel Compos. Struct.*, **32**(5), 595-610. https://doi.org/10.12989/scs.2019.33.6.805.

Schulz, U., Peters, M., Bach, F.W. and Tegeder, G. (2003), "Graded coatings for thermal, wear and corrosion barriers", *J. Mater. Sci. Eng.: A*, **362**, 61-80. https://doi.org/10.1016/S0921-5093(03)00579-3.

Semmah, A., Heireche, H., Bousahla, A.A. and Tounsi, A. (2019), "Thermal buckling analysis of SWBNNT on Winkler foundation by non local FSDT", *Adv. Nano Res.*, **7**(2), 89-98. https://doi.org/10.12989/anr.2019.7.2.089.

Shahsavari, D. and Janghorban, M. (2017), "Bending and shearing responses for dynamic analysis of single-layer graphene sheets under moving load", *J. Braz. Soc. Mech. Sci. Eng.*, **39**(10), 3849-3861. https://doi.org/10.1007/s40430-017-0863-0.

Shinde, B.M. and Sayyad, A.S. (2017), "A quasi-3D polynomial shear and normal deformation theory for laminated composite, sandwich, and functionally graded beams", *Mech. Adv. Compos. Struct.*, **4**, 139-152. https://doi.org/10.22075/macs.2017.10806.1105.

Singh, V.K., Hirwani, C.K., Panda, S.K., Mahapatra, T.R. and Mehar, K. (2019), "Numerical and experimental nonlinear dynamic response reduction of smart composite curved structure using collocation and non-collocation configuration", *Proc. Inst. Mech. En., Part C: J. Mech. Eng. Sci.*, **233**(5), 1601-1619. https://doi.org/10.1177/0954406218774362.

Soldatos, K.P. (1992), "A transverse shear deformation theory for homogeneous monoclinic plates", *Acta Mech*, **94**(3), 195-220. https://doi.org/10.1007/BF01176650.

Thai, H.T. and Kim, S.E. (2015), "A review of theories for the modeling and analysis of functionally graded plates and shells", *Compos. Struct.*, **128**, 70-86. https://doi.org/10.1016/j.compstruct.2015.03.010.

Thom, V.D., Dinh, K.N., Nguyen, D.D., Duc, H.D. and Tinh, Q.B. (2017), "Analysis of bi-directional functionally graded plates by FEM and a new third-order shear deformation plate theory", *Thin Wall. Struct.*, **119**, 687-699. https://doi.org/10.1016/j.tws.2017.07.022.

Tounsi, A., Al-Dulaijan, S.U., Al-Osta, M.A., Chikh, A., Al-Zahrani, M.M., Sharif, A. and Tounsi, A. (2020), "A four variable trigonometric integral plate theory for hygro-thermo-mechanical bending analysis of AFG ceramic-metal plates resting on a two-parameter elastic foundation", *Steel Compos. Struct.*, **34**(4), 511-524. https://doi.org/10.12989/scs.2020.34.4.511.

Vel, S.S. and Batra, R.C. (2004), "Three-dimensional exact solution for the vibration of functionally graded rectangular plates", *J. Sound Vib.*, **272**, 703-730. https://doi.org/10.1016/S0022-460X(03)00412-7.

Vo, T.P., Thai, H.T., Nguyen, T.K., Inam, F. and Lee, J. A (2015), "A quasi-3D theory for vibration and buckling of functionally graded sandwich beams", *Compos. Struct.*, **119**, 1-12. https://doi.org/10.1016/j.compstruct.2014.08.006.

Zaoui, F.Z., Ouinas, D. and Tounsi, A. (2019), "New 2D and quasi-3D shear deformation theories for free vibration of functionally graded plates on elastic foundations", *Compos. Part B*, **159**, 231-247. https://doi.org/10.1016/j.compositesb.2018.09.051.

Zenkour, A.M. (2006), "Generalized shear deformation theory for bending analysis of functionally graded plates", *Appl. Math. Model.*, **30**, 67-84. https://doi.org/10.1016/j.apm.2005.03.009.

Zenkour, A.M. (2007), "Benchmark trigonometric and 3-D elasticity solutions for an exponentially graded thick rectangular plate", *Appl. Math. Model*, **77**, 197-214. https://doi.org/10.1007/s00419-006-0084-y.

Zhao, N., Qiu, P. and Cao, L. (2012), "Development and application of functionally graded material", *Adv. Mater. Res.*, **562-564**, 371-375. https://doi.org/10.4028/www.scientific.net/AMR.562-564.371.

CC